Gravel beach profile response allowing for bimodal sea-states

Andrea Polidoro[1], Tim Pullen[2], Jack Eade[3] Travis Mason[4] Belen Blanco[6] and David Wyncoll[7]

[1]Engineer, Coastal Structures, HR Wallingford Ltd.: a.polidoro@hrwallingford.com
[2]Principal Engineer, Coastal Structures, HR Wallingford Ltd.: t.pullen@hrwallingford.com
[3]Coastal Process Scientist, Channel Coastal Observatory, National Oceanography Centre, Southampton : jack.eade@noc.soton.ac.uk
[4]Director, Channel Coastal Observatory, National Oceanography Centre, Southampton : travis.mason@noc.soton.ac.uk
[5]Principal Scientist, Coasts & Estuaries, HR Wallingford Ltd.: b.blanco@hrwallingford.com
[6]Senior Scientist, Flood Management, HR Wallingford Ltd.: dpwyncoll@googlemail.com

Published in Proceedings of the Institution of Civil Engineers – Maritime Engineering, 2018

Abstract

The south coast of the UK is identified as a location where significant wave swell components are present within the regional wave climate. During the winters of 2006 and 2014, several sites along the south coast of the UK were subject to significant damages where flood events were recorded. These sea states were characterised by having a double-peaked wave spectra, observing a connection between wave spectrum shape and beach response. A two-dimensional (2D) physical model study was carried out to investigate the effect of gravel beach profile response under wave spectra characterised by swell-wave and wind-wave periods in various combinations. The physical model results showed the effect of bimodal wave spectrum on beach crest erosion and were compared with the parametric model Shingle and the numerical model XBeach-G. Based on this 2D physical model study, a new parametric model, Shingle-B, was derived and an online tool developed and made available on the website for the National Network of Regional Coastal Monitoring Programmes of England. This new tool has been validated at two sites in the south of England where field data of both waves and profiles were available.

Keywords
coastal engineering, granular materials, maritime engineering

Notation

$D_{x\%}$ grain size that exceeds by size x% of the sediment distribution

D_{50} median grain size

H_{m0} wind wave height

H_{m0i} significant incident spectral wave height

L_{m0} mean wavelength

$L_{m-1,0}$ deep water wave length

m_0	total spectral energy
Q_p	peakedness parameter
$S(f)$	incident spectral density
$S\%$	swell percentage
s, s_0, s_{m0}	wave steepness
$T_{m0,2}$	mean spectral wave period defined using the zeroth and second moments of the frequency spectrum
$T_{m-1,0}$	spectral wave period defined using the inverse and zeroth moments of the frequency spectrum
T_p	peak wave period
y	wind wave spectral shape
β_i	corresponding regression coefficients to be estimated when fitting
ε	broadness parameter
v	narrowness parameter
ξ_0	breaker parameter

1. Introduction

Gravel beaches are a particular type of beach in which the sediments are solely composed of gravel sediment (2mm to 64mm, according to the Wentworth scale, Folk scheme, BGS, 1987) according to Lopez de San Roman Blanco (2003). It is also common to find coarse grained beaches which include both gravel and mixed (sand and gravel) sediments.

These beaches are common in mid to high latitude coasts (Carter and Orford, 1993; Horn and Walton, 2007; Hayes et al., 2009) but also present on the shores of many parts of the world. Gravel beaches assume particular importance, as defence systems, along stretches of the heavily populated South coast of England where they are known as shingle beaches (Nicholls, 1990; Moses and Williams, 2008). Approximately one-third of the beaches in England and Wales are classified as coarse grained, especially along the south coast of England (Blanco, 2001). A gravel beach can be seen as a sum of different zones where the interaction of hydrodynamic processes and beach characteristics influence the final response of the beach. These zones are schematised in Figure 1.1. The most important zones for these beaches are the surf and swash zone. The surf-zone is the zone of wave action extending from the water line out to the most seaward point of the zone where waves start breaking (breaker zone). In the surf-zone, the sediments will be subject to a complex set of forces which are produced due to bed friction and the impact of the breakers, which generates significant turbulence and sediment sorting. The surf-zone is a very dynamic zone and the response of the beach profile is extremely linked to a change of the incident wave energy. The swash zone is the zone of wave action on the beach, extending from the limit of run-up to the limit of run-down. As discussed in more detail in Horn (2002), the interaction between wave motion and beach groundwater table (see Figure 1.1) provides an important control on swash zone sediment transport.

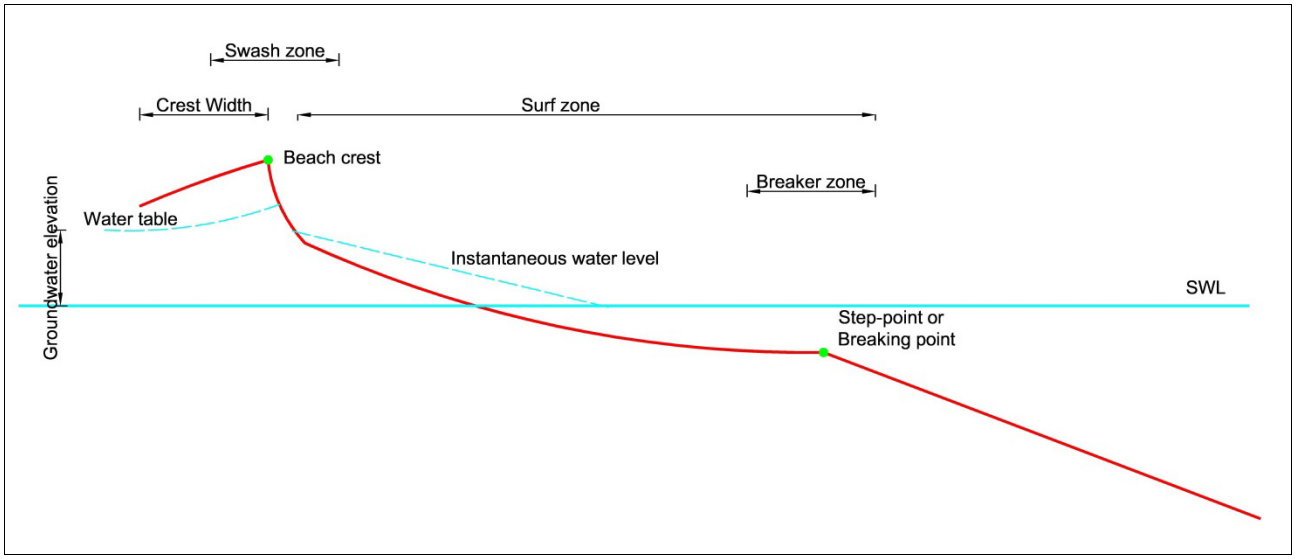

Figure 1.1: Schematisation of a general beach profile

Gravel beaches are an important form of natural coastal defence, protecting significant urban settlements as well as agricultural, recreational and environmental land areas against flooding and erosion (van Wellen et al., 2000; Powell, 1990). Their functions as coastal defences and natural habitats therefore compels coastal engineers to understand the processes occurring across the gravel beach face (Buscombe and Masselink, 2006). The beach behaviour is coupled with the incident wave conditions, hence the need for coastal engineers to study the approaching wave climate in order to have a reliable prediction of the beach response. In South coast of England, it is common to have Atlantic swell waves penetrating into the English Channel (up to about Beachy Head) leading often to wave conditions with a broad, bimodal (combination of wind a swell wave components) or multi-modal spectrum (Bradbury *et al*. 2007). Along the south coast of the England a significant presence of bimodal sea-states are recorded. Typical sites affected by the bimodal conditions are: Milford-on-Sea, Hayling Island, Rustington, Boscombe, Chesil, West Bay and Penzance (Bradbury *et al*., 2007).

The impact of wind waves on the coast in terms of overtopping, beach erosion, armour damage, etc., are relatively well understood for many simple configurations (van der Meer, 1988; Powell, 1990; EurOtop 2007). Conversely, swell waves, having longer periods than wind waves (Goda, 2010), are not generally considered in coastal structures design. However, it is possible that a combination of wind-sea and swell waves represent a worst case sea-state for some aspects of beach design (Bradbury, 2006). Indeed, recent work carried out by Thompson *et al.* (2017) noted that bimodal sea-states lead to greater overtopping and that the formulae available in literature underestimate wave overtopping under bimodal wave conditions. An example of the effect of the bimodal sea-states on the coastlines was observed during the winters of 2006 and 2014, where several sites along the south coast of the England were subjected to significant damage due to flooding events. Total economic damage for England during the winter period was estimated to be between £1000 million and £1500 million, including the damage due to fluvial and groundwater flooding (DEFRA, 2016). A programme of nearshore wave measurement, wave hindcasting and beach response to extreme storm events in the English Channel, observed that bimodal (double-peaked) wave conditions produced more damage to the beaches than suggested by empirical models (based on statistical wave parameters) (Bradbury *et al*., 2002; 2004; 2007). In particular, the beach responses related to the measured wave data during these events suggested that the unexpected beach behaviour and breaching phenomena was linked to the spectral characteristics of the storm events (Bradbury, 2007). Interestingly, these

sea-states were characterised by having moderate rather than storm wave conditions, and their wave spectra presented a notable energy within low frequencies (Mason *et al*, 2008). Subsequent to these storm events, a correlation between bimodal wave spectra, beach response and breaching events was identified.

A 2D physical model study carried out by Hawkes (1998) confirmed the critical impact of long period energy influencing the beach response, however, during that study a predictive method was not developed. Hawkes (1998) states that, following the results of the study, the existing method of predicting beach response could be inadequate when bimodal conditions are present.

Similar conclusions were confirmed by Bradbury (2007 et al.) who observed that bimodal conditions significantly affect the beach profile performance, influencing the impact of wave run-up, erosion and overwashing. They also emphasised the need to consider bimodal wave conditions as a design variable for some areas of the English Channel coast.

Unfortunately, still little is known about the effect of bimodal sea conditions on sea defences or beaches (Coates and Bona, 1997; Bradbury, 1998; Bradbury, *et al*., 2007) and swell is rarely considered explicitly in the design or assessment of shoreline management operations. Indeed, as it will be described in more detail in the following sections, the use of the existing prediction models for gravel beach profiles (Powell, 1990) known as SHINGLE, and the process-based XBeach-G (McCall *et al*., 2014) are not appropriate tools for bimodal conditions. This is because these prediction models are based on experiments carried out with simple unimodal sea-states, neglecting the possibility of having the complex wave conditions that combine wind wave and swell, forming a bimodal spectrum. There was therefore an urgent need to better understand the effect of the interaction between wind wave and swell waves on the beach response and developing our understanding of the prediction of beach response under bimodal storm conditions.

The objective of this study was to develop a new parametric model for predicting beach profile response of shingle beaches under bimodal wave conditions in order to increase confidence in beach cross-section design. An empirical framework, based on extensive 2D physical model data and field work was developed to examine the profile response of gravel beaches to bimodal wave spectra, characterised by swell and wind wave periods in various combinations. Based on this 2D physical model study, a new parametric model, Shingle-B, for predicting gravel beach profile response has been derived. This model is available online on the website for the National Network of Regional Coastal Monitoring Programmes of England (http://www.channelcoast.org/ccoresources/shingleb/).

This paper discusses both the results of the physical model and the development of a parametric model, which represents an improvement over existing models for gravel coasts, subjected to bimodal wave conditions. Section 2 provides a more detailed description of bimodal sea-states. The 2D physical model study and its results are discussed in Section 3 and Section 4, respectively. The existing predictive methods for shingle beach morphological response are reviewed in Section 5 and applied to some of the physical model experiment results. The new parametric model, Shingle-B, is described in Section 6.

2. Occurrence of bimodal sea-states

The presence of bimodal (double-peaked) wave spectra has been observed along several coasts of the globe, e.g., Atlantic and Pacific Oceans (Garcia-Gabin, 2015), the west coast of New Zealand (Ewans, 2006) and the Gulf of Mexico and Southern California (Mackay, 2016). In particular, in the south coast of England, Atlantic swell waves penetrate into the English Channel often leading to wave conditions with a broad, bimodal or multi-modal (having several maxima) spectrum (Bradbury *et al*. 2007). The swell propagates up the English Channel reaching the coastline east of the Isle of Wight, and occasionally, it can extend the full

length of the English Channel (Mason *et al* 2008). Analysis of wave spectra from the National Network of Regional Coastal Monitoring Programmes' coastal wave network has identified that bimodal sea conditions occur on a regular basis (Mason *et al.,* 2008). Typically, the highest presence of bimodal seas is associated with sites exposed to Atlantic swell e.g. Porthleven in Cornwall. The occurrence of bimodal seas is seasonal, being more common during the winter months (December, January, and February) and less common in the summer (June, July and August) as shown in Figure 2.1, where an average seasonal percentage of bimodal wave conditions recorded during the period from July 2003 to July 2016 is reported.

The effect of long period waves on gravel beaches in the South coast of England was already observed in the past. A typical example is Hurst Spit, which during its life, was breached several times, and the spit was indeed breached several times between 1983-84. The most severe damage, however, occurred on 16 and 17 December 1989, when southwesterly storms combined with a surge in excess of 1 m flattened an 800 m length of Hurst Spit (Wright, D, 1998), as shown in Figure 2.2.

More recently, during the winter of 2013 – 2014, the south coast of England was exposed to an unusual and prolonged combination of severe storms. Many sites in central southern England experienced between 5 and 7 storms during this winter period (October 2013 to February 2014). A number of storms exceeded the extreme wave conditions of 1 in 10 year, or 1 in 50 year return periods as shown in Figure 2.3, where the geographical occurrence/location of recorded return period exceedance between October 2013 and February 2014 is shown. Analysis of a 60-year hindcast wave model record (validated by offshore wave buoy measurements) by Masselink et al. (2016) suggests that the 2013/ 2014 winter was the most energetic since 1948. The storm sequences during the winter of 2013 to 2014 along the south coast of England had a considerable impact on many of the beaches. During these storms, Hurst Spit was subject to an unpredicted breaching (see Figure 2.4), and in many other parts of the south coast of England, flooding and overwash events were observed.

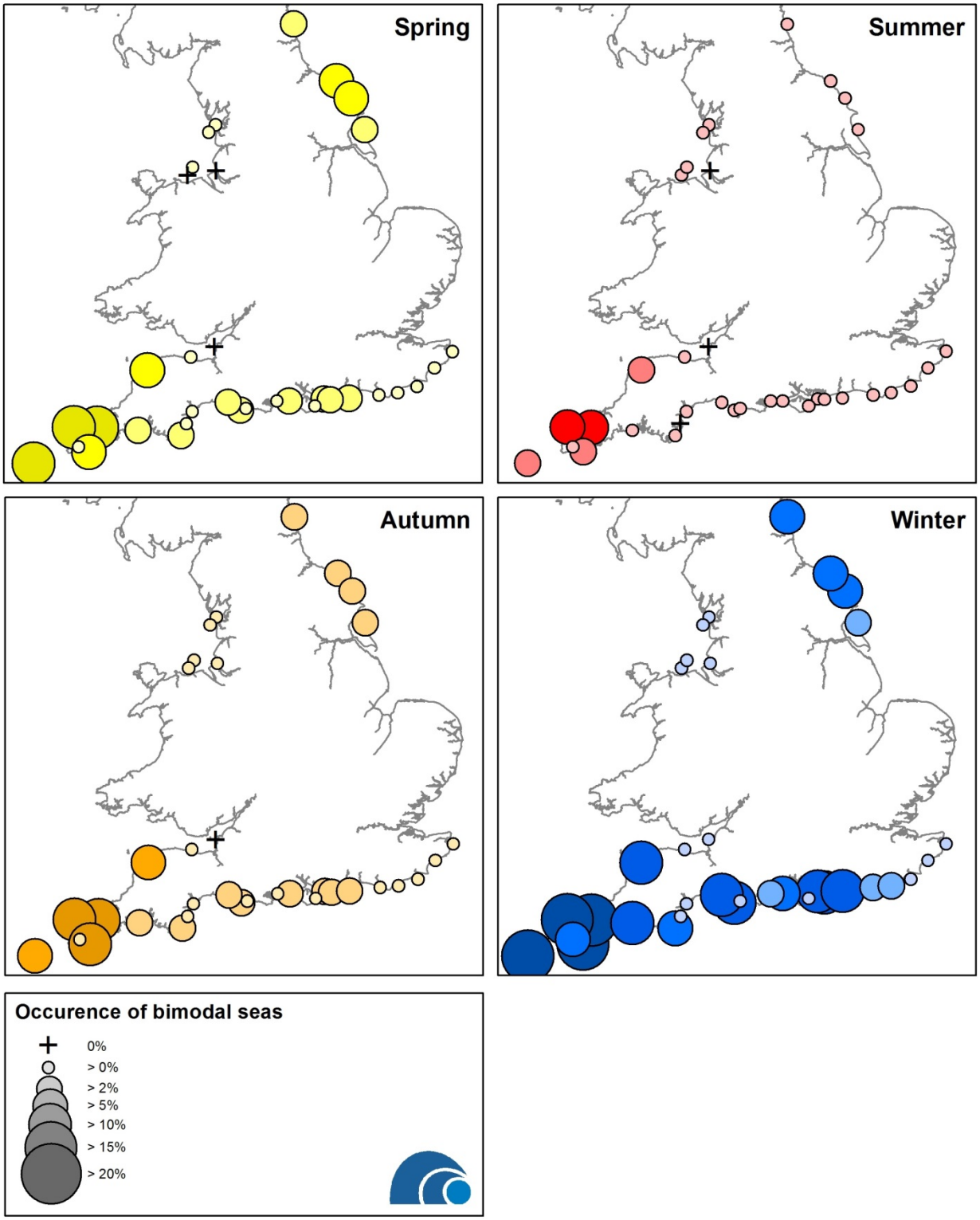

Figure 2.1: Seasonal occurrence of bimodal seas (Extracted from Channel Coastal Observatory study, 2018)

Figure 2.2: Hurst Spit, breached in 1989, @NFDC

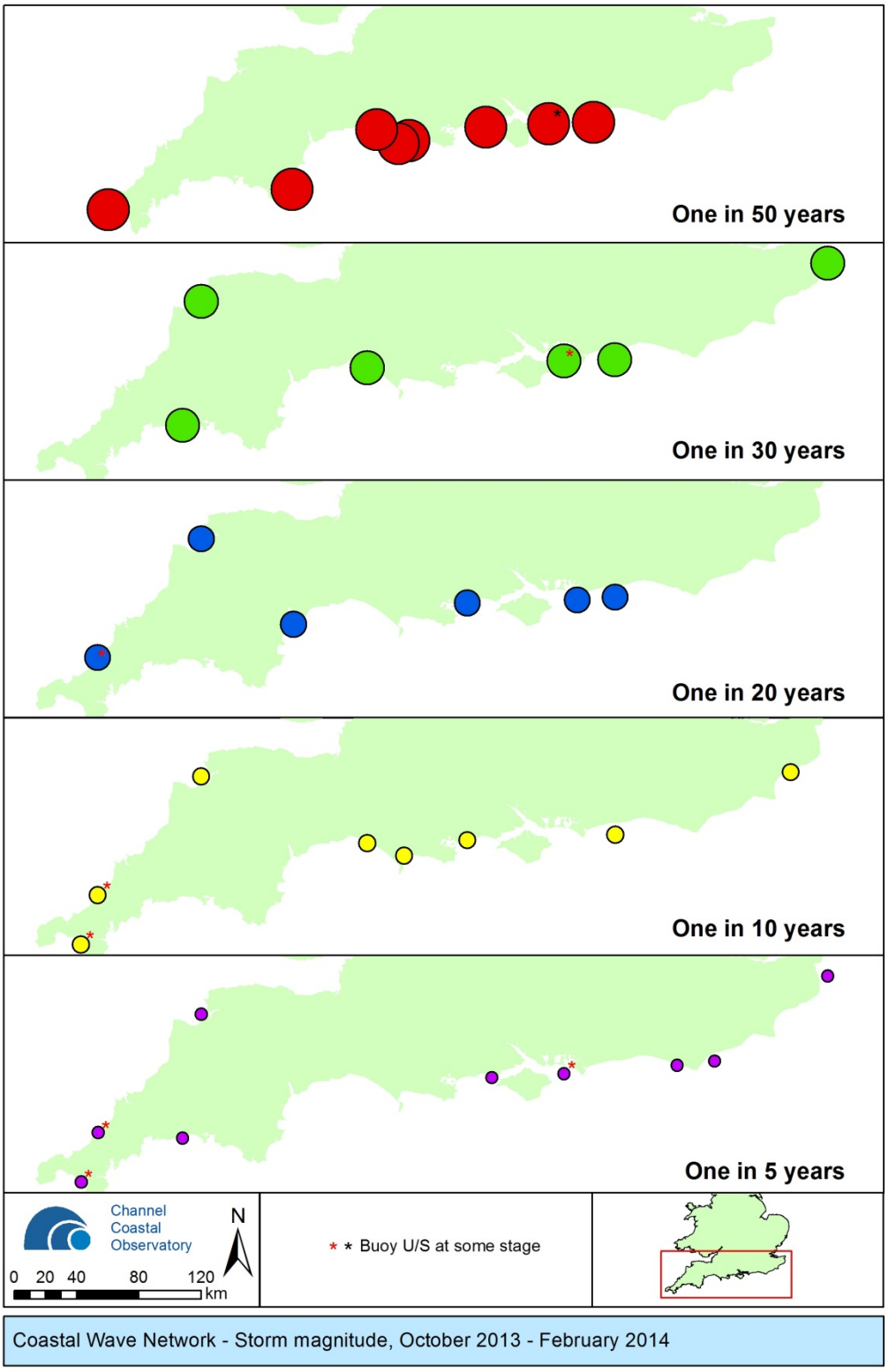

Figure 2.3: Distribution of storms exceeding the 1 in 5 year return period between October 2013 and February 2014 (Extract from, A. Bradbury & T. Mason, Report SR 01, April 2014)

Figure 2.4: Hurst Spit, unpredictably breached in 2014, (Courtesy Peter Ferguson @NFDC)

The driving force behind this new research, however, has its roots in less stormy bimodal conditions. A sequence of unexpected (not forecasted) coastal flooding events were observed at Seaton, Cornwall, in October 2006 and at Hayling Island on 03 November 2005. All these instances were recorded during periods of moderately, rather than stormy, wind wave conditions, but notable for the underlying presence of long period swell waves (Mason *et al*., 2008). Figure 2.5 shows Seaton during one of these unpredicted flooding events in October 2006. As it can be seen in the figure, the flood-gate had remained open during the flooding event, highlighting the fact that the wind wave forecast alone was unable to predict the potential for flooding.

For the present study, the bimodal half-hourly spectra recorded at Chesil, Milford, Rustington and Hayling Island, from January 2005 to September 2015, have been used to extract the occurrence of the swell percentage on the total wave energy spectrum. The spectra were obtained from the National Network of Regional Coastal Monitoring Programmes, and the results are shown in Figure 2.6, where it can be seen that for a bimodal wave spectrum, the swell component percentage ranges between 10% to 70%. Most of the bimodal wave spectra present a swell component between 10% and 20%, but cases of swell between 30% and 50% are common. In some cases, bimodal spectra with 70% of swell component have also been recorded. As discussed in more detail in the following section, the wave conditions tested in the 2D physical model consisted of swell percentages ranging between 10% to 40%, as these represent the vast majority of all the sea-states analysed.

Figure 2.5: Seaton beach, Cornwall, 2006, the flood gate remains open during the flooding event (@NFDC)

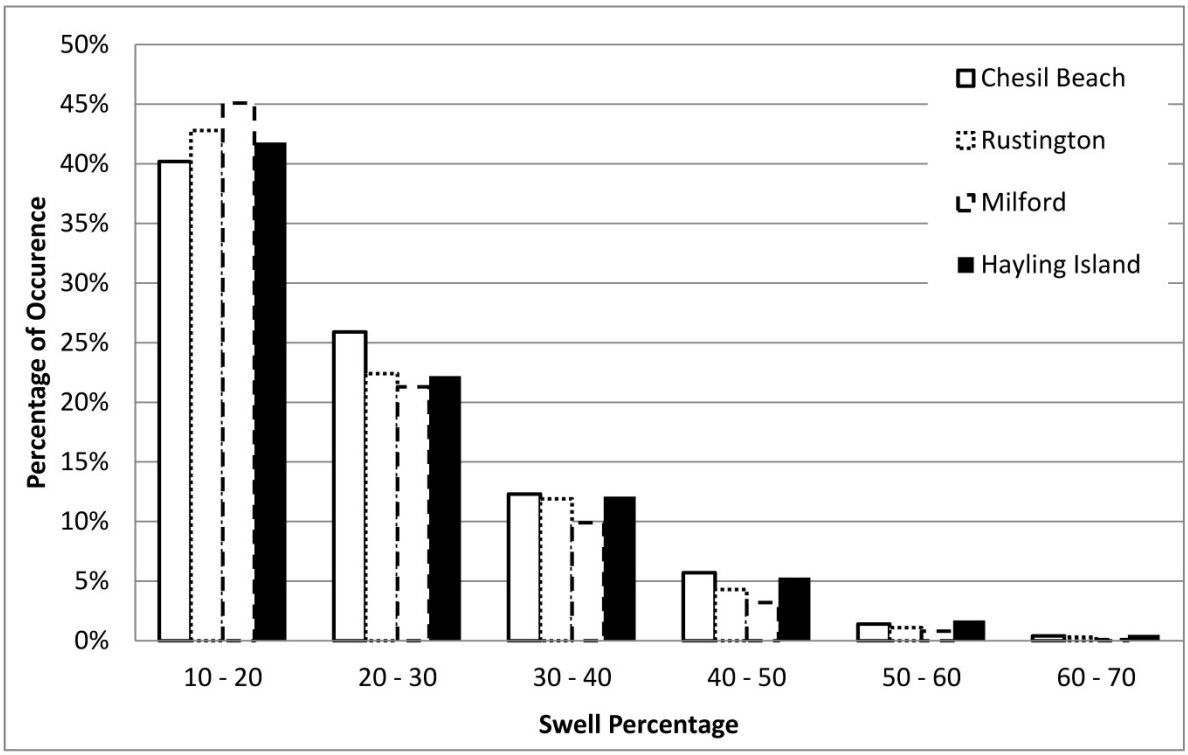

Figure 2.6: Swell percentage occurrence for the bimodal wave spectra recorded during the period from 2005 to 2015

3. Physical model study

3.1. Introduction

A 2D physical model study was carried out using a 100 m long wave flume at HR Wallingford, with a wave paddle able to generate non-repeating random sea-states to any required spectral form, including bimodal spectra. The model setup is schematised in Figure 3.1 (model scale 1 in 25), where the location of the tested gravel beach and wave probes are shown. In order to correctly reproduce the prototype beach response, the model material has to be scaled accordingly to the three main criteria described in Powell (1990). The methodology used to scale the gravel material is outlined here, with further detail in Polidoro *et al*. 2015.

The three criteria defined by Powell (1990) needed to produce the correct beach response in a mobile bed physical model study, are: the permeability of the beach (Yalin, 1963) (controls the beach slope); the relative magnitudes of the onshore and offshore motion (Dean, 1973, 1985) (controls whether the beach erodes or accretes); and the threshold of sediment motion (Komar and Miller, 1973; 1975) (hence the onset of onshore-offshore transport).

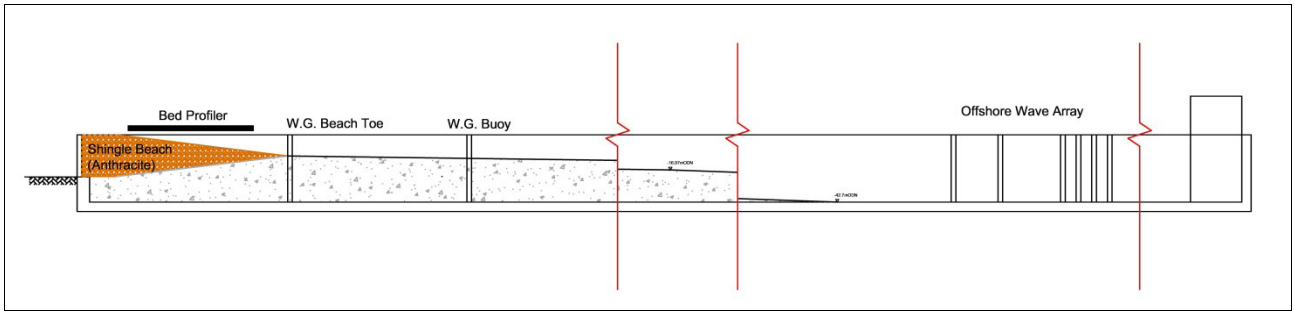

Figure 3.1: Model flume setup. Note the flume is 100m long

A study of the sediment distributions for a typical range of gravel beaches along the south coast of England, was carried out by Powell (1993). Based on Powell's work, a typical grading curve (D_{50} = 12.5 mm and D_{10} = 2.8 mm) was reproduced in this study by using four distinct mixes of crushed anthracite (specific gravity of 1400 kg/m^3). The anthracite used for the beach is supplied in six different grades, which were combined to achieve the model grading curve shown in Figure 3.2 (solid line) versus the target grading curve (dashed line). The use of anthracite in reproducing correctly the behaviour of a prototype gravel beach was confirmed by the comparisons between the measured test profiles from the Großen Wellen Kanal (GWK) (Blanco *et al*, 2006) with the profile predicted by SHINGLE (Powell, 1990). The good agreement between predicted and measured profiles, generally indicated that the methodology previously adopted by Powell (1990) for small-scale testing of shingle beaches (use of anthracite) correctly describe the cross-shore profile response under normally incident wave conditions (Bradbury, 2002).

During this study, the initial beach slope was 1 in 8 (plane sloping beach) for all the test conditions, as shown in Figure 3.3. For each test, the post-storm beach profile was measured using a 2D bed profiler, which extracted the profile elevation every 20mm along the x-axis. The bed profiler was mounted above the central section of the beach, enabling coverage of a 4m (model) long profile across the mobile sediment. The touch-sensitive probe has a proximity switch which allows it to detect the bed with the minimum of contact pressure. The probe is stepped forward and lowered down on the bed; the encoder in the profiler then determines the bed height. This probe is particularly suitable for profiling both below and above the water surface. The bed profiler was used to monitor all tests with an accuracy of ± 1.0mm vertically and horizontally (the prototype scale equivalent would be 25 mm accuracy or equivalent to one piece of large gravel).

For each wave condition, described in the following section, an in-line array of six wave gauges was used to measure both the incident wind and swell waves. Time histories recorded by each gauge in the array were analysed spectrally to give the following parameters: significant incident spectral wave height, H_{m0i}, peak wave period, T_p; the mean spectral wave period, $T_{m0,2,}$ defined using the zeroth and 2nd moments of the frequency spectrum; and the spectral wave period, $T_{m-1,0}$, defined using the inverse and zeroth moments of the frequency spectrum. The tests were carried out using a non-repeating sequence of duration equal to 3,000 times the mean wind wave period, $T_{m0,2}$, of the target spectrum.

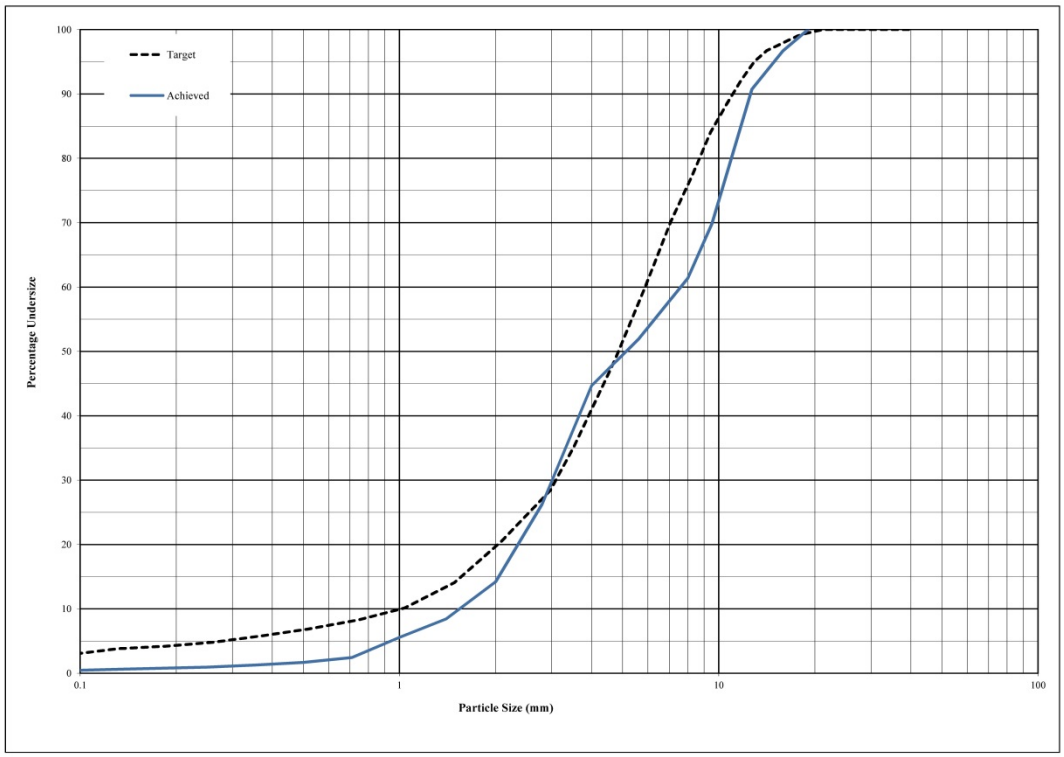

Figure 3.2: Target grading curve vs model grading curve of the anthracite used in the physical model tests

Figure 3.3: View of the tested plain beach

3.2. Design wave conditions

This section briefly outlines the waves used during testing, the shape of the spectrum, range of wave periods and how these are all related to the total spectral energy (m_0). A more detailed discussion of the spectral shape is given in Polidoro *et al*. (2015).

The principal purpose of this study was to cover a large range of input conditions to examine the response of shingle beaches under bimodal sea-states, where design wave attack is assumed to be normal or near normal. The wave conditions were based broadly around a framework of measured conditions (wave height,

wave steepness and wave periods) derived from wave buoys at Chesil, Milford-on-Sea and Hayling Island, as described in more detail in Bradbury (2007); Bradbury *et al.* (2009) and Bradbury *et al.* (2011). Wave conditions were based broadly around prototype measurements covering a range of wave heights from 3.0m to 6.0m, swell periods from 15 to 25 seconds and wave steepness of 0.03, 0.04 and 0.05. Once the wave heights were established, the wind wave periods were changed to between 6 to 9 seconds to obtain the set wave steepness. Prototype wave conditions were defined at locations in 12 to 15 m water depth, therefore, wave measurements in the flume were made at correspondingly equivalent depths, as shown in Figure 3.1 (wave gauge buoy).

Each test was run with both a nominal wind wave and the associated idealised bimodal wave. The nominal wind wave was described by wind wave spectral shape (γ), wind wave height (H_{m0}) and wind wave period (T_p), as shown in Figure 3.4. The bimodal wave was described by a superposition of a wind wave and a swell wave, that together have the same total energy (area under the curve, [m_0]) as the nominal wind wave. The bimodal spectra is therefore predicted using the total H_{m0} (the sum of the energy in the spectrum), T_{pwind}, T_{pswell} and the percentage of the swell component (Figure 3.4). The bimodal spectrum was modelled using a standard JONSWAP spectrum with a peak enhancement factor of γ = 3.3 for the wind component. Analysis of swell waves generated off New Zealand showed that the swell spectra peaks were equivalent to the JONSWAP spectra with γ = 8 ~ 9 (Goda, 1983). This is because the swell waves have a spectra confined in a narrow frequency range and thus have a peak much sharper than that of wind waves (Goda, 2010). For the swell component, even though swell waves tend to have a narrow and peaked spectrum, a JONSWAP spectrum with enhancement factor of γ = 1.5 was selected in order for the wave paddle generator to reproduce well defined wave spectra for the low frequencies, without missing information when the wave energy was shifted from high to lower frequencies. Although the peak enhancement factor (γ) is expected to have a certain degree of influence on the beach profile response, this has not been investigated in past research studies and it is outside the remit of this study.

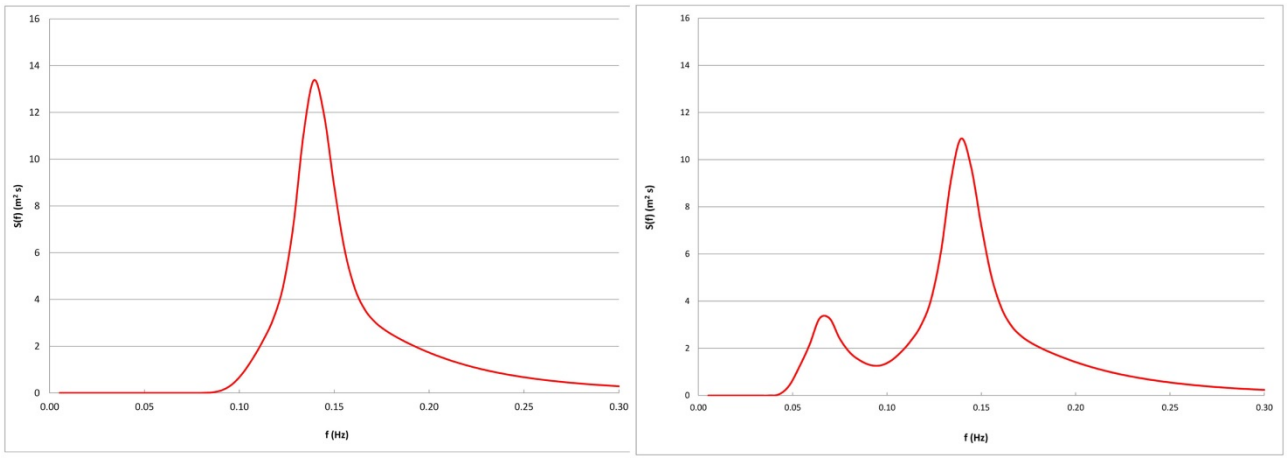

Figure 3.4: Wave spectrum: H_{m0}=4.0 m, $T_{p,wind}$=7.0 s and γ_{wind}=3.3 (left); wave spectrum: H_{m0}=4.0m, $T_{p,wind}$=7.0s, γ_{wind} = 3.3, $T_{p,swell}$ =15.0s, γ_{swell} =1.3, swell component=20% (right)

To further investigate the variation of beach profile response and wave run-up with the spectral shape and the distribution of energy across the frequencies, each wave condition was run with the same spectral wave height H_{m0}, i.e. the same area under the spectrum, and successively subdivided to represent varying percentages of swell; including 0 %, 10 %, 20 %, 30 % and 40 %. This can be observed in Figure 3.5, where the total energy under the wave spectra is maintained, although distributed with different percentage swell

components. The choice of the swell percentage was based on the work carried out by Bradbury *et al.* (2007) and the additional analysis previously discussed and summarised in Figure 2.6.

3.3. Test programme

During these tests, different combinations of wave heights and wave periods were used in four steps of varying swell percentage (10-40%) at a single water level on a 1 in 8 beach slope, with a difference in elevation between beach crest and beach toe of 17m. The tests were initially carried out with a single deep-water wave steepness s_{m0} = 0.05 and successively reduced to s_{m0} = 0.04 and s_{m0} = 0.03 in order to study the effect of wave steepness on the beach response. In addition, a fully developed swell sea-state (unimodal wave spectra,100% swell component) was run with three different swell wave periods to investigate the profile response under these conditions. A detailed description of each Test Series is described by Polidoro *et al*. 2015. Table 3.1 includes information on the order in which the Test Series were run, plus brief details on each: configuration of the shingle beach tested; the spectral wave heights and wave steepness that was run; the number of waves to reach the (dynamic) equilibrium profile and the number of tests.

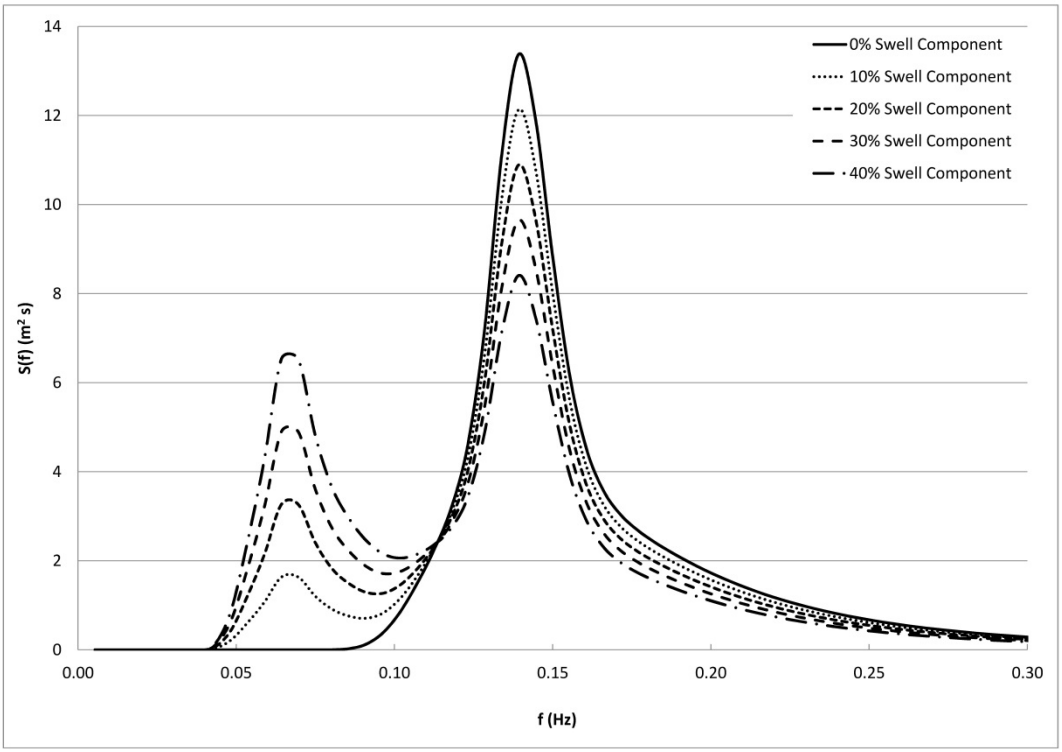

Figure 3.5: Wave spectra with different swell percentage

Table 3.1: Test Series Programme

Test Series	Beach Configuration	Wave Height (m)	s (-)	Number Waves	Purpose	No. of Tests
A	Slope 1 in 8	3.0 - 4.5 - 5.3 - 6.0	0.053	1000 - 2000 - 3000	Profile response to bimodal sea state	104
B	Slope 1 in 8	3.0	0.04	3000	Profile response to bimodal sea state	20
C	Slope 1 in 8	3.0	0.03	3000	Profile response to bimodal sea state	20
D	Slope 1 in 8	4.5	0.04	3000	Profile response to bimodal sea state	20
E	Slope 1 in 8	3.0	0.003-0.004-0.006	1000	Profile response to bimodal sea state	3

4. Physical model results

4.1. Introduction

Each test was run initially for a duration of 1000, 2000 and 3000 waves; the duration being defined by the mean wave period $T_{m0,2wind}$. Beach profiles were measured following each sequence of 1000 waves. Although the initial intention was to continue each test until dynamic equilibrium was reached, the first test results showed that after 2000 waves the profile did not change significantly (see Figure 4.1) and that there was no discernible difference after 3000 waves. It was decided, therefore, to run for 3000 waves for the remaining tests, and only profile them once at the end of testing. This is in agreement with the results obtained by Powell (1990), where it was observed that approximately 80% of the total volumetric change occurred during the first 500 waves.

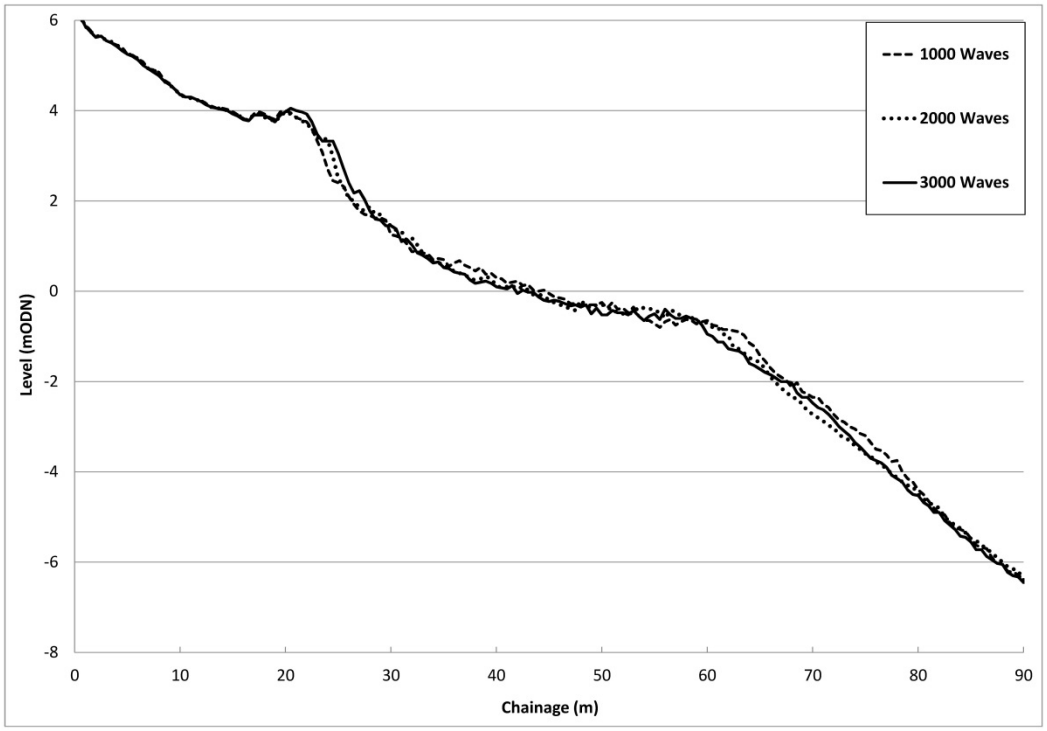

Figure 4.1: Profile development for a wave condition run for a duration of 1000, 2000 and 3000 waves (based on $T_{m0,2}$) in the physical model tests

The representation of random sea waves can be considered as a stochastic process where the whole varies randomly with time (Goda, 2010). A given sea-state, characterised by spectral energy, can be reproduced by an infinite number of time series having the same spectral energy (Goda, 2010). In order to investigate the effect of the time series sequence on the final beach profile response, four different random time series (with the same wave spectrum and different random sequences) were generated. Results of the beach profiles under these four random time series are plotted in Figure 4.2. The final profiles showed that the crest position and the lower limit of the profile developments are relatively insensitive to the sequence of the time series. However, the beach profile within the surf-zone is, as expected, slightly more sensitive to the sequence of the train of waves. This can be explained because within the surf-zone waves start breaking, and therefore non-linear responses influence the sediment transport. This part of the beach profile is very dynamic, changing almost wave by wave so that even the last sequence of waves affects the final profile. As a consequence, the final beach profile shows a small variability within the surf-zone, possibly due to the effect of the final sequence of waves. Based on these observations, throughout this study it was decided to run different time series for each test condition. The ability to generate long non-repeating time series is of great importance when testing models that have a non-linear response, as in this case.

Almost 200 profiles were recorded, and it is therefore not possible to present all of them in this section. Instead, results are presented where they assist understanding of the main outcomes or where it is necessary to illustrate trends or specific aspects of interest.

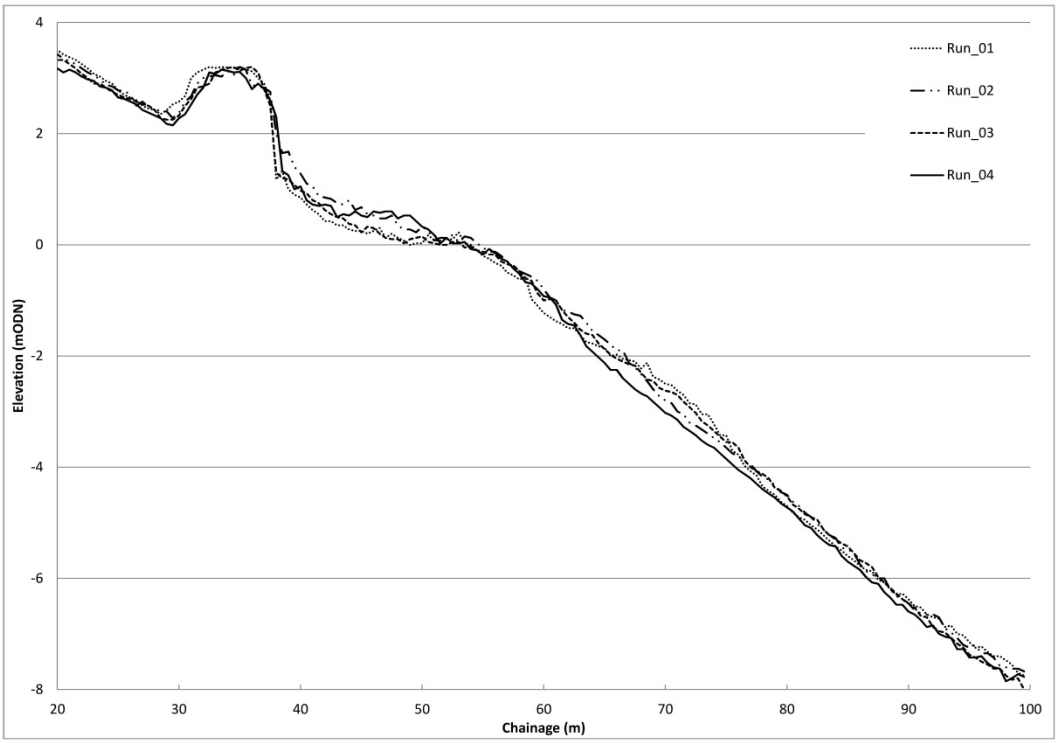

Figure 4.2: Effect of varying time series sequence on beach profile response in the physical model tests

4.2. Swell component effect on beach profile response

An example of the effect of the swell percentage on the beach profile is plotted in Figure 4.3, where wave conditions with the same swell wave period of $T_{p,swell}$ =18s, same wave height of H_{m0} = 3.0m, but different swell components are plotted. The influence of the swell component was observed mainly in the upper portion of the profile. The surf-zone width increased significantly in response to an increase of swell percentage. This can be explained by the interaction of wind and swell waves on the final beach profile evolution. During the wave motion, long swell waves run up the beach and a significant volume of water infiltrates into the beach. The amount of the water that penetrates and it is retained by the beach is also a function of the beach permeability i.e., the beach grain size distribution (which was outside the remit of this study). This will raise the groundwater elevation, which is a function of both wave conditions and sediment sizes, and obviously the tidal level, which was not considered within these experiments. If the beach is almost saturated with water, during the backwash a thick layer of water within the surf-zone will be present (see Figure 4.4). The next incoming wave will surf on top of this water layer and, as the beach is now saturated, part of its energy cannot be dissipated within the beach. Most of the wave energy is, therefore, used to run on top of the crest and push the beach crest landward. This phenomenon can be observed in Figure 4.4, where a breaking wave can be seen running on a beach already saturated with water.

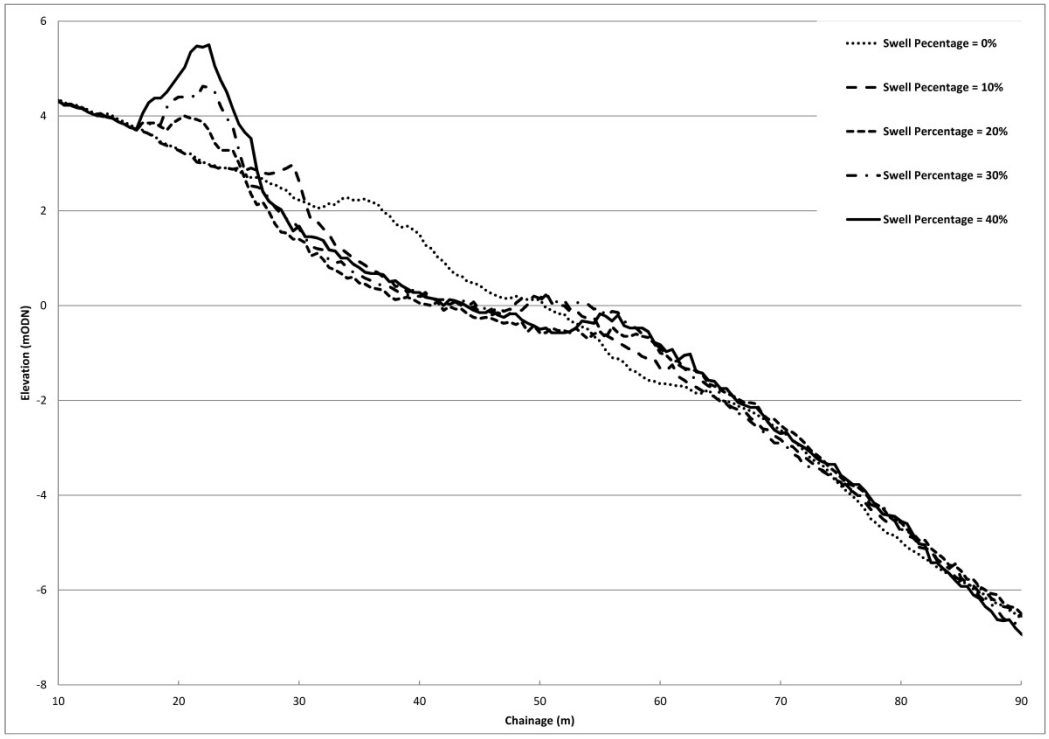

Figure 4.3: Effect of swell component percentage on shingle beach profiles (H_{m0} =3.0m, $T_{p,wind}$ =7.18s, $T_{p,swell}$ =18s) in the physical model tests

Figure 4.4: Beach saturated by the swell waves and wind waves surfing on top of the sheet of water created by the previous swell wave

Beach profile results (Figure 4.3) showed that the beach crest experienced a horizontal displacement in response to a shift of energy from high to low-frequency. Interestingly, results demonstrated that an increase of swell component higher than 20% (e.g. 30-40%) had a more significant impact on the vertical displacement of the beach crest rather than in the horizontal displacement. This suggests that an increased swell percentage (> 20%), will trigger an increase in crest-elevation, rather than a horizontal displacement of the beach crest. Similar trends were also observed for the other swell-wave periods tested (15s, 21s and 25s).

4.3. Swell wave period effect on beach profile response

The swell component tests demonstrated that the crest elevation was also affected by the swell wave period. Accordingly, the effect of the swell wave period ($T_{p,swell}$) on the beach profile was investigated by comparing profiles subject to the same wave height (H_{m0} = 3.0m), same wind wave period ($T_{p,wind}$ = 7.18s), same swell percentage (10%, 20%, 30% and 40) but different swell periods (15s, 18s, 21s, 25s). An example of the effect of the swell periods on the beach profile is plotted in Figure 4.5 (H_{m0} = 3.0m, $T_{p,wind}$ = 7.18s and Swell% = 30). Figure 4.5 shows that variations of swell wave period had a substantial effect upon the resulting profiles. The influence of the swell wave period manifested itself mainly on the beach crest, with the crest position moving backwards and the crest elevation moving vertically in response to an increasing swell wave period. Similarly, there is an increase in the crest elevation in response to an increasing swell wave period as the swell percentage is increased. For the same swell wave period, the higher the swell percentage the higher the increase of the crest elevation.

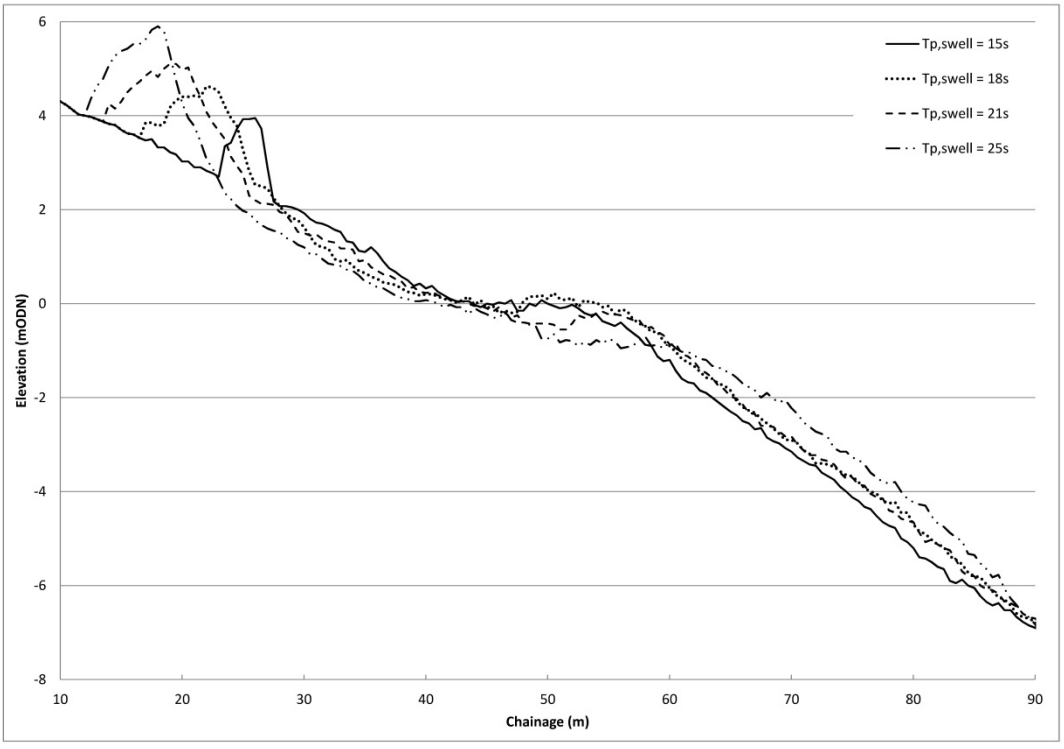

Figure 4.5: Effect of swell wave period on the shingle beach profile (H_{m0} =3.0m, $T_{p,wind}$ =7.18s; Swell percentage = 30%)

It was also observed that the breaker-zone increased in width in response to an increase of both the swell wave period and swell percentage. The increase in the width of the breaker-zone is a necessary response of the beach to dissipate increased incident wave energy but, during these wave conditions, the energy spectrum was kept constant (H_{m0} = 3.0m). This beach response may be attributed to the interaction within the surf-zone between wind and swell waves which significantly affects the run-up, run-down and groundwater elevation (see Figure 1.1), triggering an horizontal displacement (landward) of the beach crest. The effect of the groundwater elevation on the final beach profile was also discussed in Horn (2002, 2006), and it is a phenomenon extremely important for the beach evolution of coarse grained beaches in particular, although it was not investigated during this study.

4.4. Effect of wind wave period on beach profile response

The effect of the wind wave period ($T_{p,wind}$) on the beach profile was investigated for both unimodal and bimodal spectra. The beach profiles, shown in Figure 4.6, were tested under the same unimodal wave spectra, with the equivalent wave height of H_{m0} = 3.0m and different wind wave periods ($T_{p,wind}$ = 7.18s, 8.26s and 9.54s). The effect of variations in the wave period was observed more in the vertical dimension of the profile than in the horizontal displacements. Thus, as the wind wave period increases, so does the beach crest elevation. This behaviour is in agreement with the results observed in Powell (1990), where only unimodal spectra were tested.

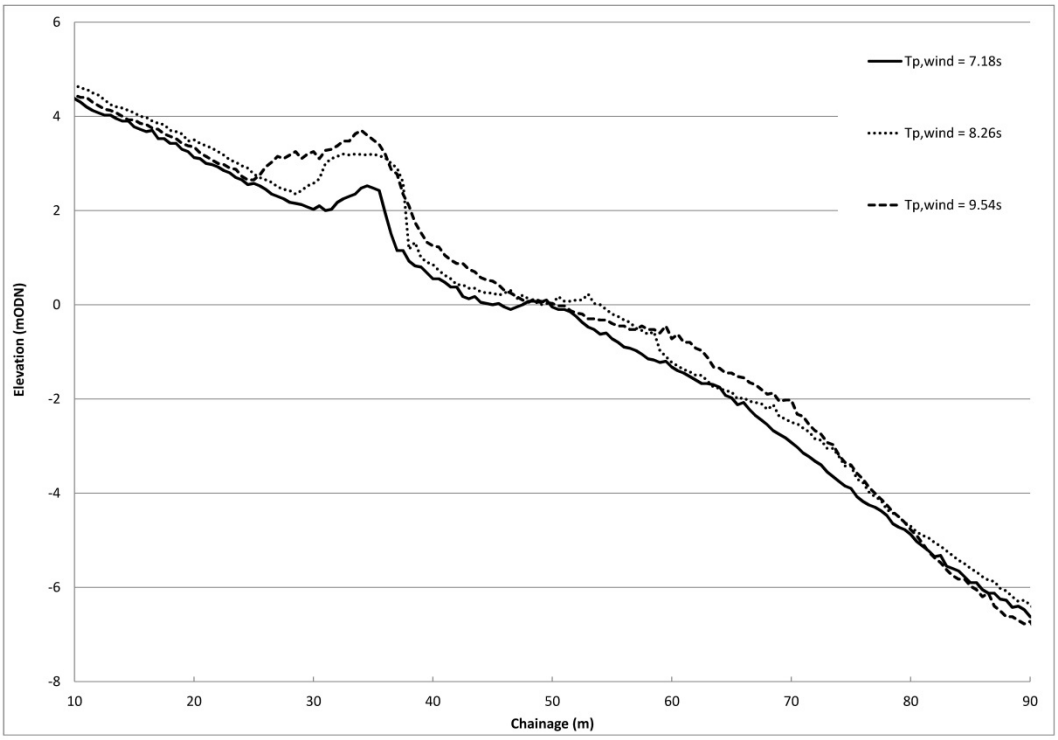

Figure 4.6: Effect of wind wave period on the shingle beach profile under unimodal wave spectra with H_{m0} = 3.0m in the physical model tests

Interestingly, under bimodal wave conditions, the increase of the crest elevation in response to an increasing wind wave period is less significant than an increase of the wind wave period under unimodal wave conditions, as shown in Figure 4.7. This plot shows four beach profiles subject to the same wave height, but

under two different wind wave periods. The profile response to unimodal wave conditions is represented with solid lines, while the profile response to bimodal wave conditions (20% swell component) are plotted with dashed lines. Clearly, the increment of the wind wave period has a more significant impact on the unimodal condition than the bimodal one. This can be explained because under the bimodal wave conditions, the swell component and swell wave period have a more significant impact than the wind wave period on the amount of water infiltrating into the beach (groundwater elevation) and therefore affecting the final profile.

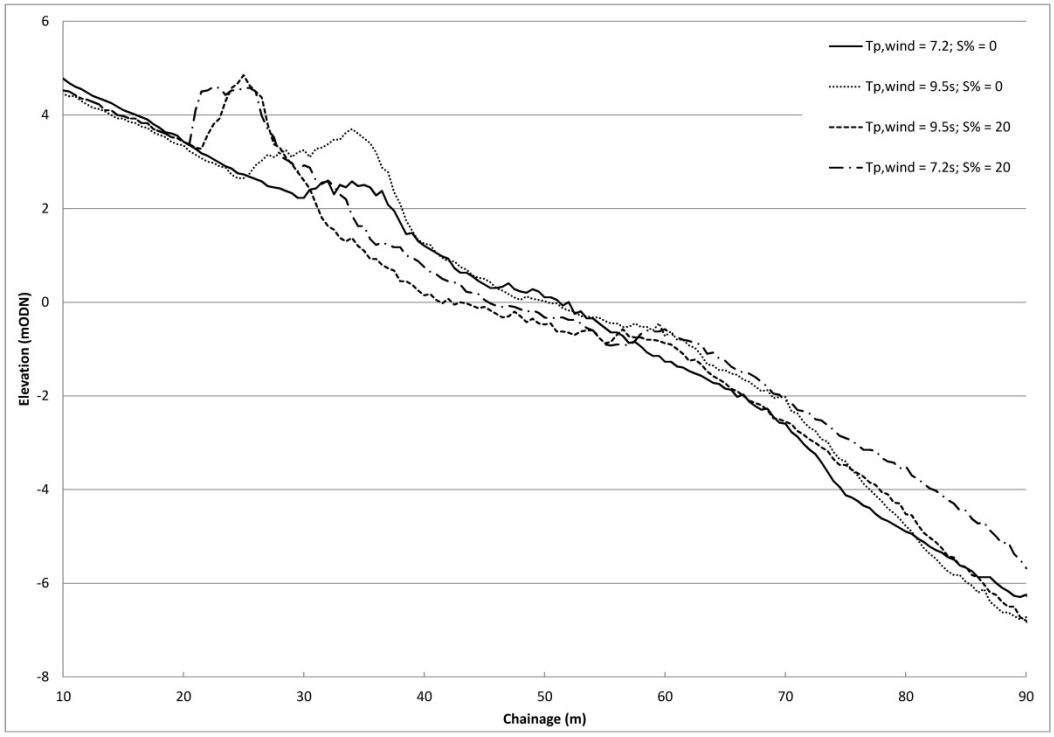

Figure 4.7: Effect of swell component on the influence of wind wave period on the shingle beach profile in the physical model tests

4.5. Wave height effect on beach profile response

The influence of the wave height on the beach profile is shown in Figure 4.8. This figure shows the post storm beach profiles exposed to two different incident wave heights (H_{m0} = 3.0m, dashed line and H_{m0} = 4.5m, solid line) having the same wind and swell wave periods. As it can be seen, the effect of the variation in the wave height triggers an horizontal displacement. The surf-zone width increases significantly in response to an increasing wave height. This behaviour is in agreement with the results observed in Powell (1990). The increase in the width of the surf-zone is necessary to dissipate increased incident wave energy, and this is realised by a lengthening of the surf-zone rather than a change of the profile. This behaviour was also observed for all the different tested wave heights.

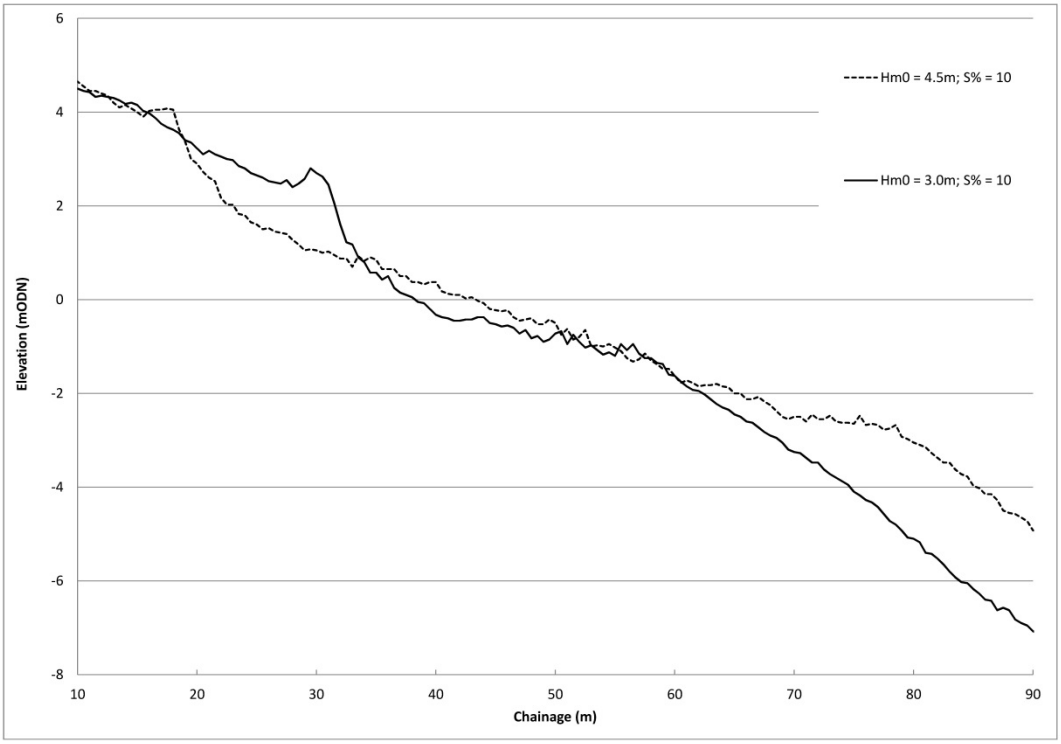

Figure 4.8: Effect of wave height on the shingle beach profile for bimodal (10% swell component) wave conditions (H_{m0} = 3.0m, dashed line and H_{m0} = 4.5m, solid line)

5. Comparison with the existing predictive methods

This section examines the main available methods used to predict gravel beach response under wave attack. The SHINGLE (Powell 1990) and XBeach-G (McCall et al., 2014) prediction models are examined by comparing the predicted beach profile responses with the physical model test results for both a typical unimodal JONSWAP wave spectrum (shown in Figure 5.1) and bimodal wave spectrum (shown in Figure 5.2 and Figure 5.3).

For a typical unimodal JONSWAP wave spectrum (H_{m0} = 3.0m, $T_{p,wind}$ = 7.18s), SHINGLE predicted profiles showing a very good correlation with the physical model results. The parametric model correctly predicted both the location of the beach crest, which tends to be the area of most interest to coastal engineers, and the location of the step (see Figure 5.1). Conversely, significant discrepancies were observed for the beach profiles predicted by XBeach-G, where the numerical model underestimated the horizontal displacement of the beach crest and predicted erosion where accretion was observed.

As previously described, in order to investigate the variation of beach profile with the spectral shape and the distribution of energy, the same spectral wave height H_{m0}, (i.e. the same area under the spectrum) was run in four additional steps of varying swell percentage (10-40%) at the same water level. Similarly, the SHINGLE and XBeach-G models were examined by comparing the predicted beach profile responses with the physical model test for a different bimodal wave spectra. In Figure 5.2 and Figure 5.3, a comparison between predicted beach profiles and the post physical model test results for bimodal wave conditions, having respectively 10% and 40% of swell component, are plotted.

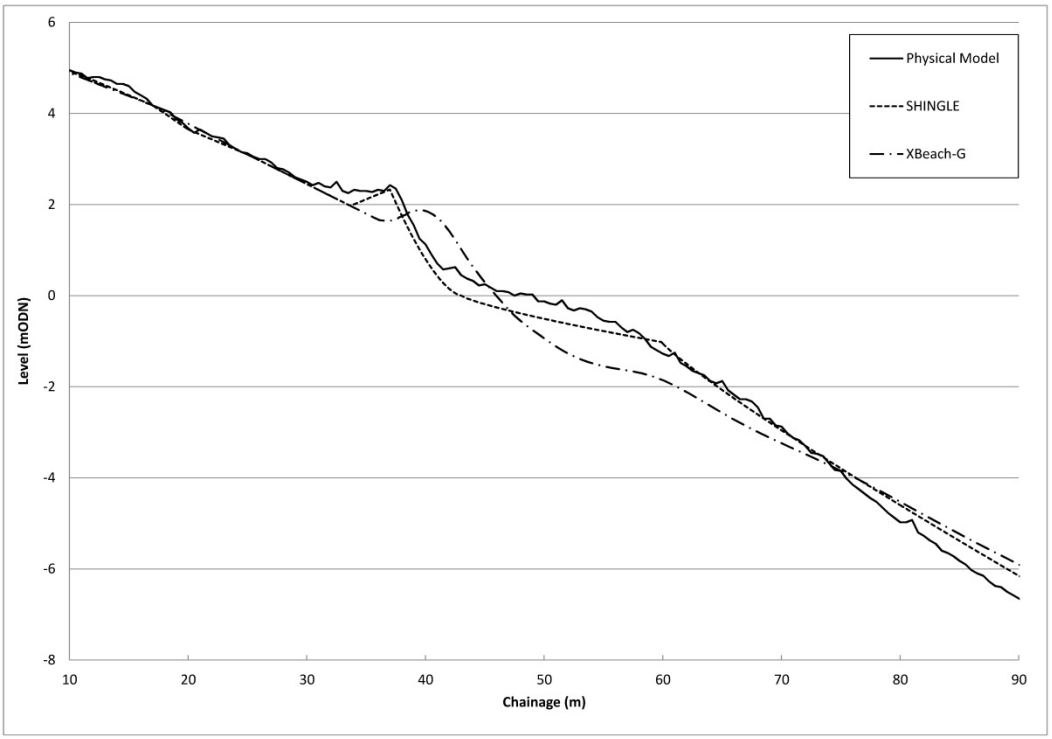

Figure 5.1: Beach profile comparison, XBeach-G, SHINGLE and physical model results for a unimodal wave spectra (H_{m0} = 3.0m, $T_{p,wind}$ = 7.18s, $T_{p,swell}$ = 15s, Swell percentage = 0%)

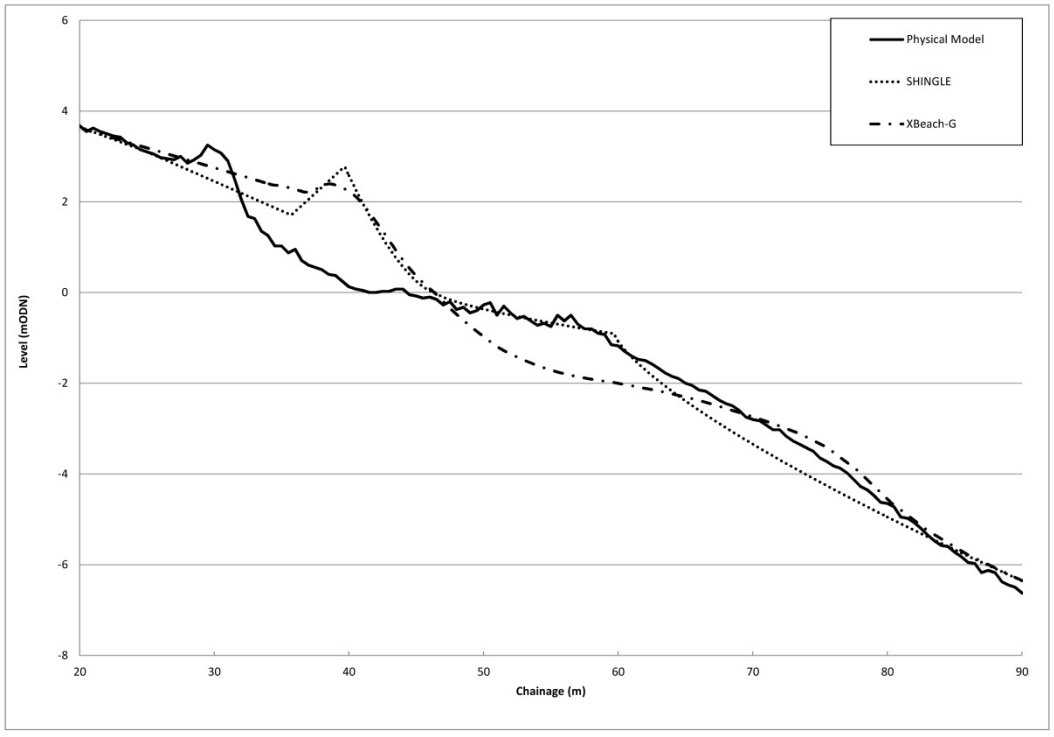

Figure 5.2: Beach profile comparison, XBeach-G, SHINGLE and physical model results for a bimodal wave spectra (H_{m0} = 3.0m, $T_{p,wind}$ = 7.18s, $T_{p,swell}$ = 15s and Swell percentage = 10%)

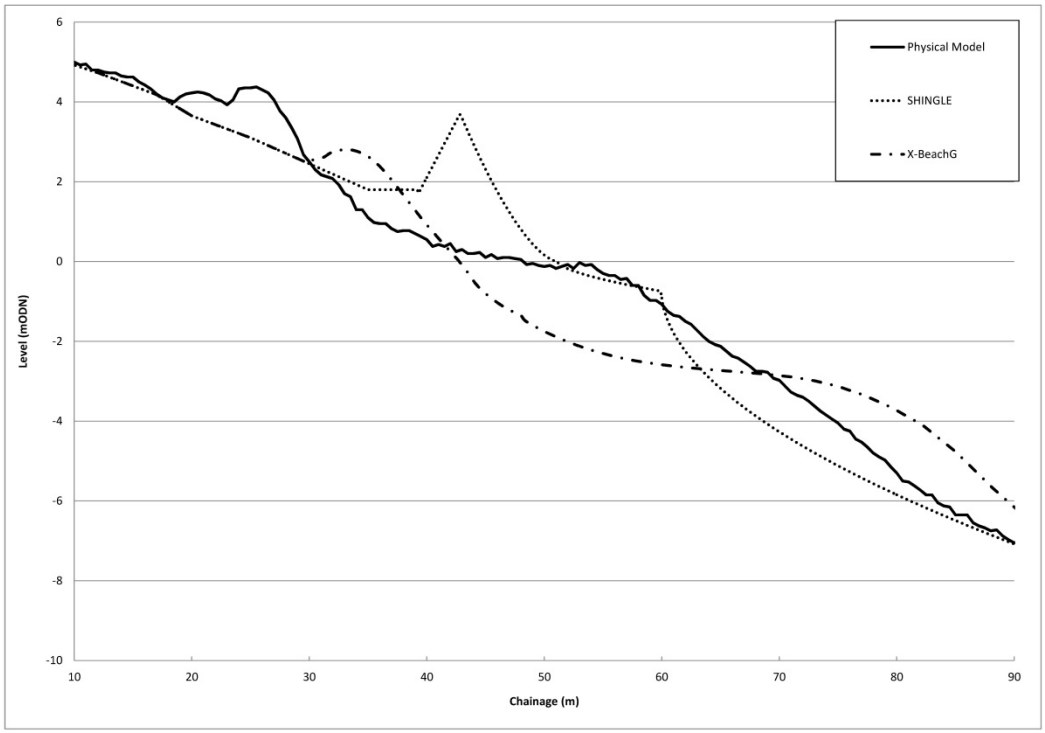

Figure 5.3: Beach profile comparison, XBeach-G, SHINGLE and physical model result for a bimodal wave spectra (H_{m0} = 3.0m, $T_{p,wind}$ = 7.18s, $T_{p,swell}$ = 15s and Swell percentage = 40%)

It is worth mentioning that the SHINGLE model allows the user to input the wave height and the mean wave period ($T_{m0,2}$), but it does not take into account the bimodality of the wave spectrum. During these tests, when varying the swell percentage (10-40%) the wave height remained constant and the spectral period ($T_{m\ 1,0}$) increased. Therefore, when increasing the swell percentage during the tests, the input mean wave period ($T_{m0,2}$) in the SHINGLE model was replaced by the spectral period ($T_{m-1,0}$). In SHINGLE, the effect of variations in the wave period triggers only the vertical displacement of the beach crest neglecting the horizontal displacement of it. As a consequence of this deficiency, a significant discrepancy between the measured and predicted profiles for bimodal wave spectra were observed, as shown in Figure 5.2 and Figure 5.3.

In contrast, in the XBeach-G model, the user is allowed to input a double-peaked wave spectrum, specifying the wave height and wave period for both wind and swell components. By comparing the measured and predicted profiles, a significant discrepancy was observed. The model does not predict the variation of the surf-zone width in response to an increase of swell percentage, and as a consequence, significantly under-estimates the crest erosion (of the order of 10 - 20m). The higher the swell percentage within the incident wave condition, the higher the discrepancy observed (see Figure 5.2 and Figure 5.3).

The laboratory experiments clearly demonstrated the effect of the double-peaked wave spectrum on the beach profile response whereby a slight increase of low-frequency energy within the incident wave spectrum, triggered a significant erosion of the beach crest. The comparison between predicted and measured beach profiles has shown that the available prediction models (SHINGLE and XBeach-G) do not encompass the effect of the bimodality of the incident wave spectrum and, consequently, they significantly under-estimate the crest erosion. Moreover, these models fail to predict correctly the width of the beach crest (seeFigure 1.1), which, as discussed in Section 2, is an important feature for the beach coastal

management. These limitations clearly indicate that the current prediction models are not appropriate tools under bimodal sea-states. Based on this 2D physical model study a new parametric model for predicting beach profile response under bimodal sea-states, Shingle-B, was derived, which is explained within the next section.

6. Shingle-B

6.1. Introduction

The first part of this section describes how new model schematises the beach profile and the relationship between profile parameters and bimodal wave variables. In the second part of this section a validation against field data is presented.

6.2. Profile schematisation

Results observed during the physical model study have shown how critical the crest erosion is during bimodal sea-states. This critical aspect of the beach profile was also observed, as discussed in Section 2, over the course of the storm sequences during the winters of 2013 - 2014 along the south coast of England. For these reasons, the profile schematisation adopted for the present model is essentially a combination of the profile employed by Powell (1990) and the necessity to predict the post-storm crest width.

Powell's (1990) model employs three power-law curves to define the shingle beach profile, as shown in Figure 6.1: 1) Beach crest and still water level shoreline; 2) Still water level shoreline and top edge of step; 3) Top edge of step and lower limit of profile deformation.

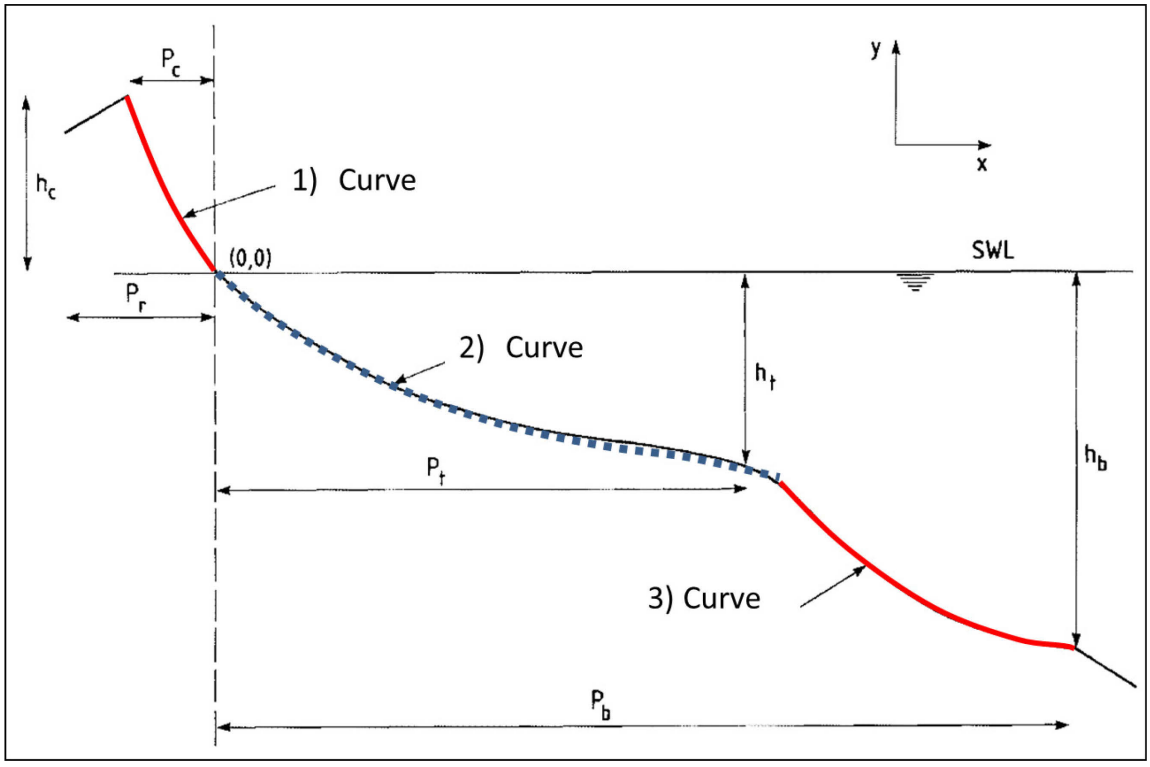

Figure 6.1: Schematised beach profile (Powell, 1990)

As discussed in Section 1, for the present model there was the necessity to predict the landward displacement of sediment and the final crest width. In contrast to SHINGLE, the suggested beach profile schematisation adopts four curves, defined by their vertices as: 1) Landward displacement and beach crest; 2) Beach crest and start beach-face point; 3) Beach-face point and top edge of step; 4) Top edge of step and lower limit of profile deformation. The resulting schematisation is shown in Figure 6.2. Except for the crest width, the parameters were measured relative to the still water level and shoreline axes, as shown in Figure 6.3. The coordinates for the vertices of the curves are denoted by x_1, y_1 to x_5, y_5, as shown in Figure 6.2.

Many authors (Keulegan and Krumbein, 1949; Bruun, 1954; Dean, 1977; Hughes and Chiu, 1981; Van Hijum and Pilarzyk, 1982; Powell, 1990) have suggested that a hyperbolic curve of the form $y = A\,x^n$ provides the best description for a profile of a natural beach, where the coefficients A and n are functions of the beach characteristics and incident wave conditions, and y and x are the vertical and horizontal displacement. During this analysis the profile curves between the vertices assumed the same hyperbolic relationship. Once the beach profile was schematised, the functional relationship for each of the parameters listed above had to be determined. The relationship between the beach profile parameters and incident wave parameters is described in the following section.

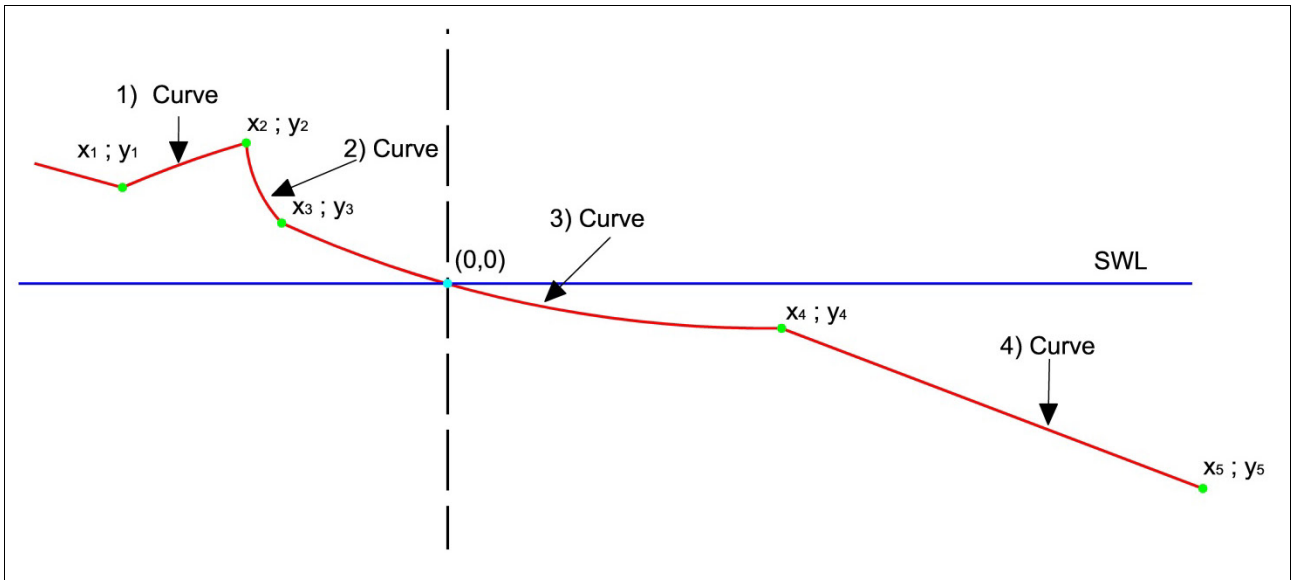

Figure 6.2: Schematised beach profile using four curves, for Shingle-B model

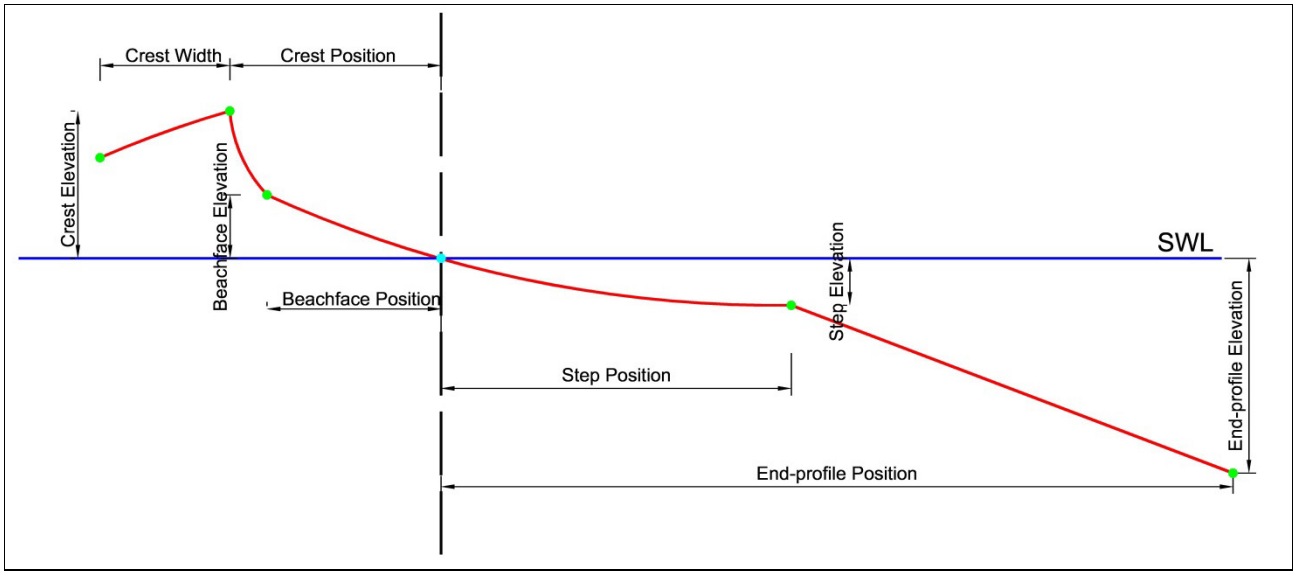

Figure 6.3: Schematised beach profile: parameters were characterised relative to the still water level and shoreline axes

6.3. Beach profile parameter identification

The physical model beach profiles were extracted using a bed profiler, (see Section 3.1) which records chainage and level at any location along the beach. In order for functional relationships between beach profile and bimodal wave variables to be extrapolated, values (co-ordinates x_i and y_i) of each of the beach parameters described above, were extracted from the beach profiles recorded during the tests (see Figure 6.4). This was done by a combination of expert judgement and a least squares optimisation.

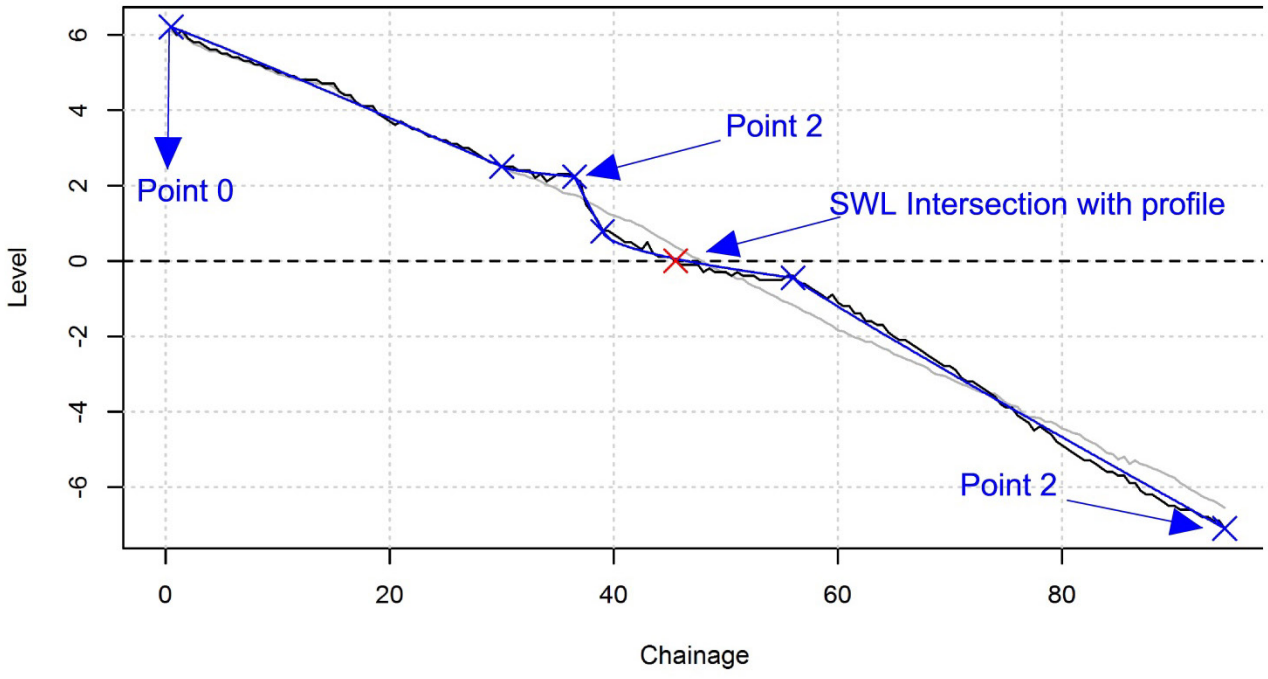

Figure 6.4: Beach parameter coordinates extracted from the physical model observed profile

Firstly, the crest position (Point 2) and still water level intersection (circle, Figure 6.4) were manually selected for each of the observed profiles. The end profile location (Point 5) was set to the end of the observed profile and an additional point (Point 0) was temporarily assigned beyond the landward limit to the opposite end to cover the whole observed profile (see Figure 6.4).

A genetic algorithm (GA) is a method for solving both constrained and unconstrained non-linear optimization problems by mirroring the natural selection process of biological evolution.

The algorithm is initialised with a population of multiple randomly generated potential solutions, each of which provides the x and y co-ordinates of the remaining beach parameters (i.e. for Points 1, 3 and 4) in addition to a power n_i for each of the six curves. This population is 'evolved' over a number of 'generations' using selection, crossover and mutation processes that mirror natural selection. At each generation, the algorithm uses the 'fitness' of each solution to determine which 'parents' used to create the 'children' of the next generation. Given a potential solution of beach parameter co-ordinates and power curves, the fitness is determined as the sum of the squared errors between the resulting fitted curves and the observed beach profile at every observed chainage, with lower errors preferred.

The resulting algorithm uses least squares optimisation to find the best fitting set of hyperbolic curves for each observed profile.

This dataset of beach parameter co-ordinates and hyperbolic curve then forms the training data for the subsequent regression analysis.

6.4. Functional relationships between beach profile and bimodal wave variables

The dataset of the observed beach parameter values, shown in Figure 6.3, with the corresponding bimodal wave variables, was used to fit the equations for predicting each parameter, and hence the profile curve, as a function of bimodal wave variables. Multiple linear regression was used to describe each profile parameter by a parametric function of potentially multiple wave variables. This gives prediction equations of the general form:

$$y = \beta_0 + \beta_1 x_1 + \beta_2 x_2$$

where y is the parameter prediction, x_i are covariates and β_i are corresponding regression coefficients to be estimated when fitting. The covariates may potentially be any bimodal wave variable or transformations of them. Test Series A to D, described in Table 3.1 (plane beach profile), were used to fit the model, ignoring the profiles at 1000 and 2000 waves, as discussed in Section 4.1.

For each profile parameter (e.g.: crest elevation, crest position, etc.), a model building exercise was undertaken to determine the exact form of the final regression equation by selecting which wave covariates to include. Finding this subset of covariates involves two opposing criteria: firstly, the regression model has to be as complete and realistic as possible, i.e., including every covariate that is even remotely related to the dependent variable; and secondly, including as few variables as possible. This is because each irrelevant covariate decreases the precision of the estimated coefficients and predicted values. Moreover, the presence of extra variables increases the complexity of the final model. The goal of variable selection becomes a balance between simplicity (as fewer covariates as possible) and fit (as many covariates as needed).

Based on the discussion above, from a selection of potential covariates, a stepwise procedure was applied whereby the simplest model with no covariates was initially chosen, then new terms were added or removed sequentially by selecting the term that minimises the Akaike Information Criterion (AIC) value (Akaike, 1974; Burnham and Anderson, 2002). AIC can be used to perform model comparisons, given a collection of models for the data. AIC is an estimator of the relative quality of statistical models for a given set of data. Thus, AIC provides a means for model selection. The process systematically adds the most significant variable or removes the least significant variable during each step. This approach measures the goodness-of-fit of the equation but penalises the number of covariates to discourage overfitting which would likely lead to poor estimates outside the fitted range (Burnham and Anderson, 2002). For each profile parameter, a set of equations were derived by the AIC method, the final one was manually selected to balance the goodness-of-fit with the model complexity while also ensuring the equation was physically meaningful (i.e. guaranteeing the physical phenomena observed and described in Section 4).

In Section 4, it was concluded that the most influential wave variables for the beach profile evolution were the spectral wave height (H_{m0}), wind wave peak period ($T_{p,wind}$), swell wave peak period ($T_{p,swell}$) and swell percentage (S). During the regression analysis, in addition to the main four variables, the following wave variables were also considered as covariates: spectral significant wave period ($T_{m-1,0}$), mean wave period ($T_{m0,2}$), mean wave length (L_{0m}), breaker parameter (ξ_0), wave steepness (s_0) and also three parameters related to the wave spectrum: broadness (ε), narrowness (ν) and peakedness (Q_p).

Ultimately, as a result of the stepwise regression analysis, the following four covariates were considered for inclusion in the regression equations: H_{m0}, S, (1-S) $T_{p,wind}$ and S $T_{p,swell}$, where S is the swell percentage as a decimal between 0 and 1. The wind and swell peak periods were multiplied by factors involving the proportion of swell to ensure that the covariate has a valid value in all cases, including when the swell is 0% or 100% for which one of these periods is undefined.

The model selection process was conducted using 90% of the selected tests with a randomly selected 10% used for independent validation of the fitted models. An example of the analysis shows the results for the crest position and crest elevation in Figure 6.5. Ultimately, the selected regression equations were refitted using all of the selected tests. The final equations describing each parameter, and hence the profile curve, as a function of bimodal wave variables are reported in Appendix A. These equations are the basis of the online beach prediction tool Shingle-B.

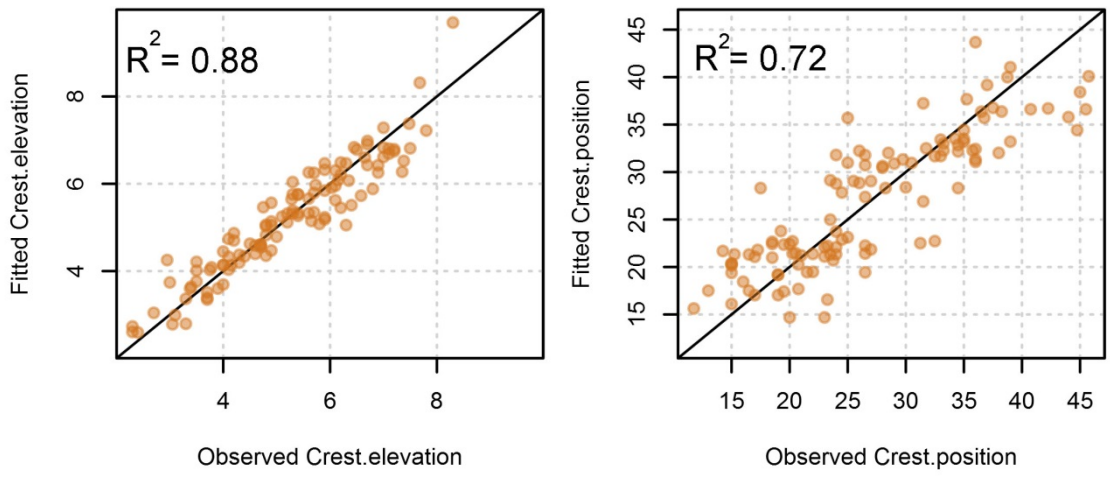

Figure 6.5: Fitted vs observed values for validation for the crest elevation (left) and crest position (right)

6.5. Model validation

The final and perhaps most important stage is the validation of the Shingle-B model against field data. This, if successful, confirms the correctness of the theory behind the beach physical modelling and generates confidence in the application of results from those models to natural situations. The following section focuses on some sites along the south coast of England and provides comparison of profile response under known storm events. At each site, nearshore directional Datawell Waveriders®, owned and maintained by the Regional Coastal Monitoring Programmes, were used to measure wave conditions throughout the survey period. The wave buoys form a national network of nearshore wave measurements and are moored in ~12 m water depths providing wave statistics on a half hourly basis.

6.5.1. West Bay

West Bay comprises East and West Beach. The East Beach consists of a very fine shingle ridged beach with sand at the water's edge (see Figure 6.6). The West Beach consists of a fine, smooth, pebbly beach, with shingle and sand at the water's edge.

:

Figure 6.6: West Bay (East Beach)

A comparison between model results and post-storm beach profiles extracted at East Beach, was carried out. Data provided by CCO's website included simultaneous wave measurements and beach profiles. A single storm with a unimodal wave spectrum was recorded during January 2011 (H_{m0} = 4.6m ; $T_{p,wind}$ = 10s ; Swell % = 0) and it was reproduced by using Shingle-B, XBeach-G and SHINGLE (Powell, 1990). The prototype post-storm profile together with the three predicted model profiles are plotted in Figure 6.7, where a reasonable agreement between measured prototype profile and Shingle-B predicted profile is observed. As expected, under unimodal wave conditions, also SHINGLE (Powell, 1990) model shows a reasonable

agreement with the prototype position of the beach crest and the rate of the crest erosion. Conversely, XBeach-G significantly underestimates the crest erosion.

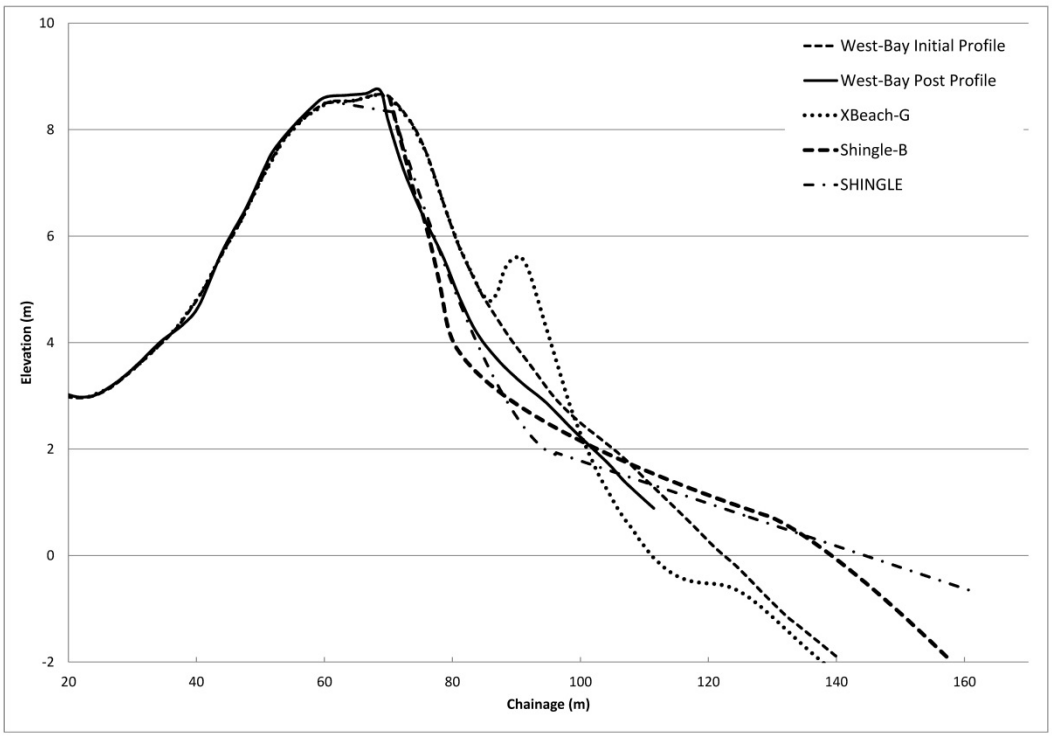

Figure 6.7: West-Bay: Post-storm profile against XBeach-G, SHINGLE (Powell, 1990) and Shingle-B predictions

6.5.2. Rustington

Rustington beach is a shingle beach with compact sand at low tide.

A comparison between model results and post-storm beach profiles extracted at Rustington, was carried out. Data provided by CCO's website included simultaneous wave measurements and beach profiles. A single storm with a bimodal wave spectrum was recorded during November 2005 (H_{m0} = 3.5m ; $T_{p,wind}$ = 7.0s ; $T_{p,swell}$ = 12s ; Swell % = 10) and it was reproduced by using Shingle-B, XBeach-G and SHINGLE (Powell, 1990). The prototype post-storm profile together with the three predicted model profiles are plotted in Figure 6.8, where Shingle-B model shows a reasonable agreement with the prototype position of the beach crest and the rate of the crest erosion. Conversely, as expected under bimodal wave conditions, both SHINGLE (Powell, 1990) and XBeach-G significantly underestimate the horizontal displacement of the crest.

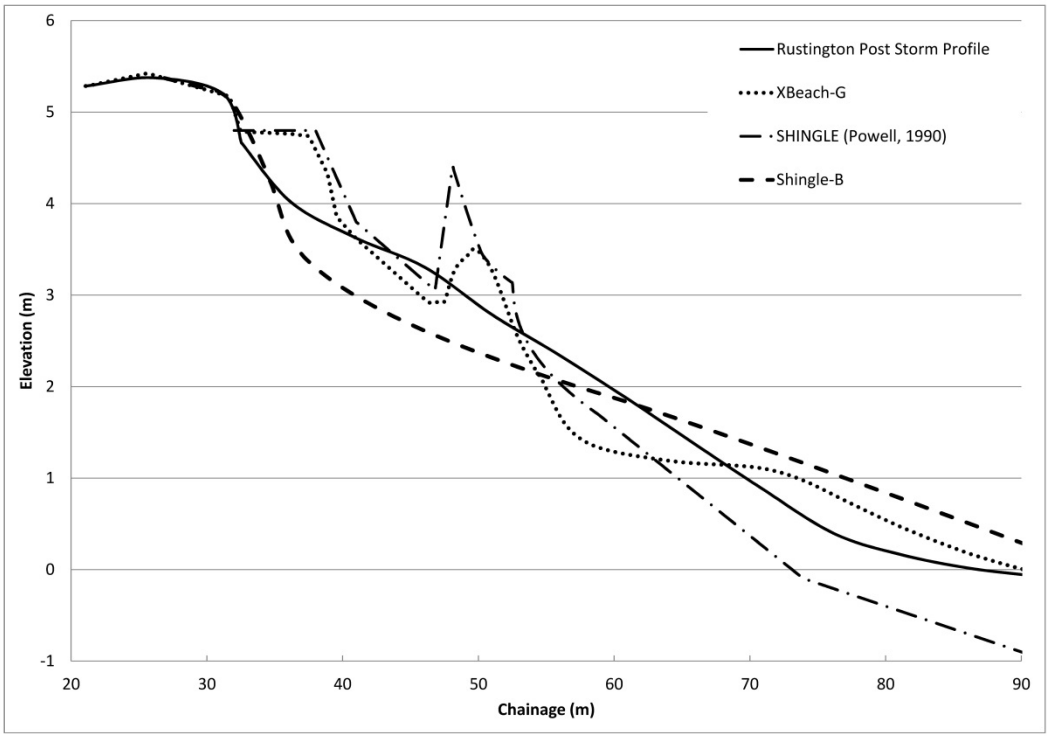

Figure 6.8: Rustington: Post-storm profile against XBeach-G, SHINGLE (Powell, 1990) and Shingle-B predictions

7. Limitations of Shingle-B

The study considered the effect of wave height (H_{m0}), wind wave period ($T_{p,wind}$), swell wave period ($T_{p,swell}$), swell percentage (S%) and the distribution of the spectral energy on the morphology of shingle beaches as a response to a storm condition.

As with all empirical methods it is important to consider the range of applicability of the model, in terms of the input parameters used for predictions. Whilst the fitted functions can provide estimates beyond the range of the data, there is little theoretical basis for their use in this regard. Although the range of the input data used to train the model could be tabulated for each of the specific input parameters, the practice of using the maximum and minimum values of each input parameter to define the range of applicability is questionable, particularly when parameters are correlated. There can be significant areas of the input parameter space unpopulated and hence predictions in these areas are generated by extrapolation not interpolation. This is illustrated in concept and for two variables only in Figure 7.1, where the parameter space covered by the maximum and minimum of two variables is given by the dashed rectangle; the orange area inside, although within the range of the variables, has no data to support the underlying predictions. This effect is significantly exacerbated the more dimensions are in the parameter space; in our case four parameters (wave height (H_{m0}), wind wave period ($T_{p,wind}$), swell wave period ($T_{p,swell}$) and swell percentage (S%).

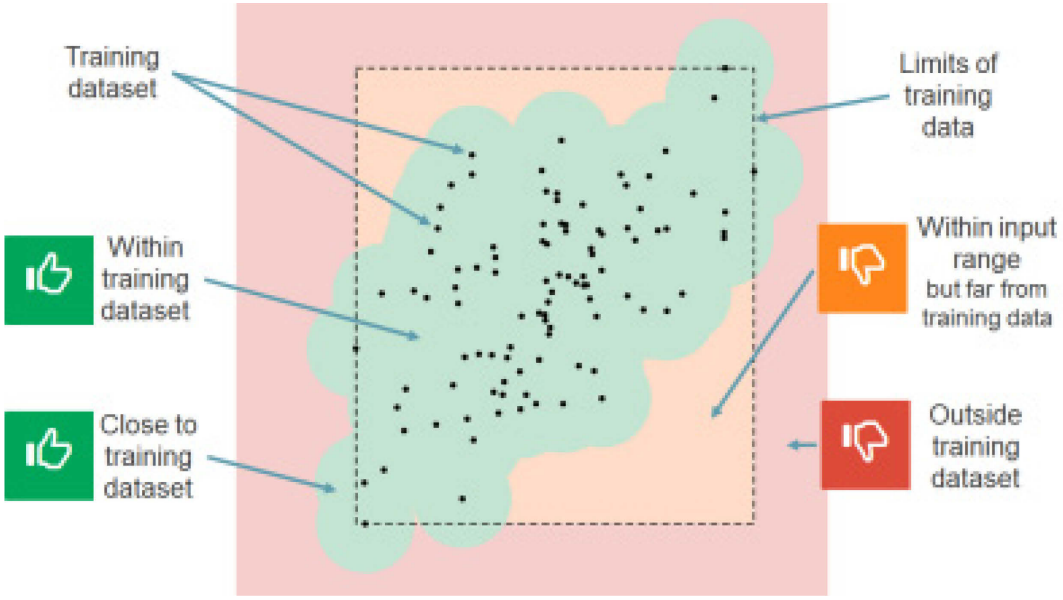

Figure 7.1: Input wave condition validation

The desire to extend the range of applicability of the model outside the range of the training data is perhaps understandable given the preponderance of existing similar structure types and the additional expense associated with constructing site-specific physical models or more sophisticated numerical models. It is however, appropriate to explicitly recognise and acknowledge that predictions resulting from extrapolation should be treated accordingly. Within the approach described here, specific attention has been directed towards the provision of guidance relating to the area of applicability of the model. The Mahalonobis Distance (Mahalonobis, 1930) provides a quantifiable measure that can guide users on regions of valid application. The Mahalanobis Distance (MD) is a measure of a point from a multivariate distribution. Unlike Euclidean Distance (ED), the Mahalanobis Distance accounts for correlated parameters, an important factor in the development of gravel beach profiles. In the online tool Shingle-B, the Mahalanobis distance has been used as a measure to come up with a range of applicability. This has been represented in the tool as a coloured thumb which is shown to indicate if the input wave conditions are within the limits of the training dataset (green thumb), within input range but far from the training data (orange thumb) or outside the data range against which the model was trained (red thumb). This is also illustrated in Figure 7.1.

It is worth mentioning that the model Shingle-B is not a breaching model nor does it deals with structures. Shingle-B only deals with the cross-shore profile; the longshore transport not being considered. Formulations such as van Wellen *et al*, 2000 should be used in order to deal with the longshore transport of coarse grained beaches. Future physical modelling tests should include oblique wave attack and the inclusion of longshore sediment transport.

7.1. Bathymetry

While a fixed bathymetry seawards of the toe of the beach, typical of south coast beaches, was used sites with extensive shallow foreshores will require some transformation of the wave conditions to determine more realistic input conditions. Such sites will likely have higher wave heights at the toe of the beach. Also, for other sites around the world, where more complicated bathymetry of the beach might be present, the user

will be therefore required to adjust the Shingle-B input wave conditions to account for the difference in bathymetry.

7.2. Diameter and grading of the beach material

Sediment characteristics such as D_{50} and grading width (D_{85}/D_{15}) may affect the beach profile response. During this study, only one grading curve was used (D_{50} = 12.5 mm, D_{10} = 2.8 mm and D_{85}/D_{15} = 5.0) for the physical model tests; this was representative of south coast beaches, as discussed in Section 3. The sediment used within the physical modelling was scaled following Yalin (1963) in order to provide the most satisfactory reproduction of the prototype beach permeability, sediment mobility threshold and onshore-offshore transport characteristics (Powell, 1990). The scaling process results showed that the sediment model scale (anthracite), with a geometric scale of 1 in 25, should be 1 in 2.25. The grading of the beach material, which affects its permeability, may influence crest elevation and crest regression, however this effect was not explored during this study. The effect of the grading of the beach on the crest elevation was studied by Powell (1990), who observed decreasing crest levels for narrower grading curve, although insufficient data were available to confirm this trend.

7.3. Beach slope

During this study, the initial beach slope in the physical model tests was fixed at 1 in 8 for each of the tests. Although the effect of the slope was not investigated, different wave conditions were repeated without reshaping the beach to the initial plane profile. Results of non-reshaped and reshaped profiles showed a very good agreement suggesting that the initial profile does not significantly affect the final profile.

Similar results were also discussed in Powell (1990) where it was concluded that whilst the initial beach slope does not necessarily affect the form of the active length of beach profile it does affect its development.

7.4. Underlying impermeable structure

Physical model tests were run with a full thickness of beach material and the effect of impermeable membrane or sea walls was not considered during this study. The presence of an underlying impermeable layer within a shingle beach was investigated by Powell (1990). During this study (Powell, 1990) it was observed that if the ratio of effective beach thickness to median material size (D_{50}) was less than 30, the thickness of the beach was usually insufficient to retain material over the profile, and the beach structure was not stable.

8. Conclusions

An extensive series of physical model tests was undertaken to explore the behaviour and performance of gravel beaches under bimodal wave conditions. The tests considered the effect of the wave height, wind wave period, swell wave period and swell component percentage on the resultant beach profiles. Results from this study clearly demonstrated the effect of bimodal spectral on the evolution of the beach profile. Test results have shown the critical effect of the bimodal sea-state on both the vertical / horizontal displacement of the beach crest and the dynamic of the surf-zone.

SHINGLE model (Powell, 1990) and the numerical model XBeach-G (McCall et al, 2014) were found not to account for the influence of the spectral shape on the beach profile response and significantly underestimated the crest erosion under the bimodal wave conditions.

The physical model results have allowed the development of a new parametric model, Shingle B, for predicting beach profile response on gravel beaches under bimodal sea-states. Using the new parametric model, an online tool was developed and made available on the website for the National Network of Regional Coastal Monitoring Programmes of England. (http://www.channelcoast.org/ccoresources/shingleb/). The new model, Shingle-B, aims to represent an engineering tool to increase confidence in beach cross-section design under wave conditions characterised by double peaked spectrum.

Initial validation of the model predictions against field data yielded encouraging results, suggesting that the parametric model provides a good representation of natural beaches, and therefore representing an improvement over existing models for gravel coasts, subjected to bimodal wave conditions. However the present model would benefit from some additional comparisons and verification with field data.

Acknowledgements

This project was the brainchild of Professor Andy Bradbury, whose untimely death in August 2014, in the middle of the experiments, deprived the coastal engineering community of one of its foremost experts on gravel beaches. The authors are also grateful to Keith Powell for guidance and supervision.

The authors also wish to acknowledge support provided by the HR Wallingford Froude Modelling Hall staff. Shingle-B was funded by the Environment Agency as a flood and coastal erosion risk management grant in aid project, grant no. LDW 4123.

Appendix

$$\text{Crest width } = 3.92 + 0.31\ \mathrm{ST_{p,swell}} \quad (1)$$

R^2 = 0.24

$$\text{Crest position} = -8.80 + 9.10\ \mathrm{H_{m_0}} + 0.66\ \mathrm{ST_{p,swell}} \quad (2)$$

R^2 = 0.72

$$\text{Crest elevation.} = -1.88 + 0.81\ \mathrm{H_{m_0}} + 0.31\ (1 - \mathrm{S})\mathrm{T_{p,wind}} + 0.37\ \mathrm{ST_{p,swell}} \quad (3)$$

R^2 = 0.88

$$\text{Beachface position.} = -11.66\ + 8.63\ \mathrm{H_{m_0}} + 0.52\ \mathrm{ST_{p,swell}} \quad (4)$$

R^2 = 0.67

$$\text{Beachface elevation} = -0.65 + 0.71\ \mathrm{H_{m_0}} + 0.12\ \mathrm{ST_{p,swell}} \quad (5)$$

R^2 = 0.56

$$\text{Step point position} = -17.76 + 8.67\ \mathrm{H_{m_0}} + 0.83\ \mathrm{ST_{p,swell}} \quad (6)$$

R^2 = 0.55

$$\text{Step point elevation.} = -1.19 + 0.51\ H_{m_0} + 0.06\ ST_{p,swell} \quad (7)$$

R^2 = 0.42

$$\text{End profile elevation} = 12.23 \pm 1.50\ H_{m_0} \quad (8)$$

R^2 = 0.54

References

Akaike, H., 1974. A new look at the statistical model identification. IEEE Transactions on Automatic Control 19: 716–723.

BARDEX: a large-scale laboratory study of gravel barrier dynamics. Special Edition - Coastal Engineering Volume 63, May 2012.

Bradbury, A.P. (2000) Predicting Breaching of Shingle Barrier Beaches-Recent Advances to Aid Beach Management. Proc. 35th. Annual MAFF Conference of River and Coastal Engineers.

Bradbury A.P., McFarland S., Horne J and Eastick C., (2002) Development of a strategic coastal monitoring programme for southeast England (*International Coastal Engineering Conf, Cardiff, ASCE*

Bradbury A.P., Mason T.E. and Holt M.W., (2004) Comparison of the Performance of the Met Office UK-Waters Wave Model with a Network of Shallow Water Moored Buoy Data, 2004 - Proc. 8th International Workshop on Wave Hindcasting and Forecasting, Hawaii

Bradbury, A.P., Mason, T.E., Poate, T., (2007). Implications of the spectral shape of wave conditions for engineering design and coastal hazard assessment - evidence from the English Channel. Presented at the 10th International Workshop on Wave Hindcasting and Forecasting, 11-16 Nov. 2007, Oahu, Hawaii.

Bradbury A.P., Mason T.E and Picksley (2009) A performance based assessment of design tools and design conditions for a beach management scheme. Proceedings of the International Conference on Breakwaters, Structures and Coastlines ICE; Edinburgh in press

Bradbury, A.P., Mason, T.E., (2014) Review of south coast beach response to wave conditions in the winter of 2013-2014. Channel Coastal Observatory, SR01.

Bruun, P., 1954. “Coast erosion and the development of beach profiles”. US Army Corps of Engrs, BEB, TM-44.

Burnham KP, Anderson DR (2002) Model selection and multimodel inference: a practical information-theoretic approach, 2nd edn. Springer, New York

Cartwright, D.E., Longuet-Higgins, M.S., 1956. The statistical distribution of the maxima of a random function. Proceedings of the Royal Society of London. Series A, Mathematical and Physical 237, 212–232.

CCO, 2008. Channel Coastal Observatory [WWW Document]. URL http://www.channelcoast.org/ (accessed 2.16.11).

CIRIA, CUR, CETMEF (2007). The Rock Manual. The use of rock in hydraulic engineering (2nd edition). C683, CIRIA, London.

Coates,T.T., and Bona, P.F.D., (1997). Recharged beach development, a field study at Highcliffe Beach, Dorset. Report SR438, HR Wallingford.

Deb, K., Pratap, A., and Agarwal, S.. A Fast and Elitist Multiobjective Genetic Algorithm: NSGA-II. IEEE Transactions on Evolutionary Computation, 6 (8) (2002), 182-197.

Deb K, Agrawal S, Pratap A, T Meyarivan, (2000). A fast elitist non-dominated sorting genetic algorithm for multi-objective optimization: NSGA-II. Proceedings of the 6th International Conference on Parallel Problem Solving from Nature.; 849-858

DEFRA (2008) Understanding Barrier Beaches. TR FD1924.

Defra (2016). The Costs and Impacts of the Winter 2013 to 2014 Floods; UK Government: London, UK, February 2016.

Dean, R.G., 1977. “Equilibrium beach profiles: US Atlantic and Gulf coasts”. Univ delaware, Dept of Civil Engrg. Report No 12.

EurOtop 2007. European Manual for the Assessment of Wave Overtopping. Pullen, T, Allsop, N.W.H. Bruce, T. Kortenhaus, A. Schüttrumpf, H. and Van der Meer, J.W. At: www.overtoppingmanual.com.

Ewans, K. Bitner-Gregersen E., Soares C. G., 2006 “Estimation of Wind-Sea and Swell Components in a Bimodal Sea State” November 2006 Journal of Offshore Mechanics and Arctic Engineering 128(4)

Garcia-Gabin, W. 2015. “Wave Bimodal Spectrum based on Swell and Wind-sea Components” IFAC-PapersOnLine Volume 48, Issue 16, 2015, Pages 223-228

Goldberg, D., 1989. Genetic algorithms. Addison-Wesley, Reading, MA.

Goda, Y. 1976. On wave groups. Proc. BOSS’ 76 (Trondheim, 1976), pp. 115-128.

Goda, Y., (1985). Random seas and design of maritime structures. University of Tokyo Press, Tokyo.

Goda, Y., 2010. Random seas and design of maritime structures, 3rd ed, Advanced Series on Ocean Engineering. World Scientific.

Hawkes P.J., Coates T.T. and Jones R.J., (1998). Impact of Bi-modal seas on Beaches and Control Structures. Report SR507, Hydraulics Research, Wallingford, copy available on request.

Hughes, S.A and Chiu, T., S., 1981. “Beach and dune erosion during severe storms”. Univ. of Florida. Coastal and Oceanographic Engrg. Dept. Report No. TR/043.

IAHR 1989 List of sea-state parameters Journal of Waterway, Port, Coastal, and Ocean Engineering Vol 115, No 6. pp 793-808.

Keulegan, G. H. and Krumbein, W.C. , 1949. “Stable configuration of bottom slope in shallow water and its bearing on geological processes”. Trans Amer geophys Union, 30, No 6.

Longuet-Higgins M. S (1983). On the Joint Distribution of Wave Periods and Amplitudes in a Random Wave Field. DOI: 10.1098/rspa.1983.0107.

Lopez de San Román-Blanco, B.L. de, 2001. Morphodynamics of Mixed Beaches (Unpublished transfer MPhil/PhD Report). Civil and Environmental Engineering Department, Imperial College, London.

López de San Román-Blanco, B., Coates, T., Holmes, P., Chadwick, A. J., Bradbury, A., Baldock, T., Pedrozo-Acuña, A., Grüne, J. (2006). Large scale experiments on gravel and mixed beaches: experimental procedure, data documentation and initial results. Coastal Engineering 53 (4), 349-363.

Mackay, E., 2016 “A unified model for unimodal and bimodal ocean wave spectra”, International Journal of Marine Energy Volume 15, September 2016, Pages 17-40

Mason T., Bradbury A., Poate T. & Newman R., 2008. Nearshore wave climate of the English Channel – evidence for bi-modal seas. Proceedings of 31st International Conference on Coastal Engineering, American Society of Civil Engineers; 605-616

Masselink, G., Castelle, B., Scott, T., Dodet, G., Suanez, S., Jackson, D., Floc'h, F., 2016. Extreme wave activity during 2013/2014 winter and morphological impacts along the Atlantic coast of Europe. Geophys. Res. Lett. 43.

McCall, R.T.,Masselink, G., Poate, T., Roelvink, J.A., Almeida, L.P., Davidson,M., Russell, P.E., 2014. Modelling storm hydrodynamics on gravel beaches with XBeach-G. Coast. Eng. 91, 231–250.

McCall, R.T., Masselink, G., Poate, T.G., Roelvink, J.A., Almeida, L.P., 2015a. Modelling the morphodynamics of gravel beaches during storms with XBeach-G. Coast. Eng. 103, 52–66.

Ochi, MK, and Hubble, EN (1976). “Six Parameter Wave Spectra”, Proc 5th Coastal Eng. Conf., ASCE, Honolulu, pp.301-328.

Polidoro, A., Dornbusch, U., Pullen, T., 2013. Improved maximum run-up formula for mixed beaches based on field data. ICE Coasts, Marine Structures and Breakwaters Conference, Edinburgh, pp. 389–398.

Polidoro, A., Pullen, T., Powell, K., 2015. Modelling Shingle Beaches in bimodal Seas, Test methodologies & Test programme. HR Wallingford report CAS1217-RT001-R03-00, UK.

Powell, K.A., 1990. Predicting Short TermProfile Response for Shingle Beaches. Hydraulics Research Limited, Wallingford, Oxfordshire. Report SR 219.

Powell, K.A., 1993. Dissimilar sediments: Model tests of replenished beaches using widely graded sediments. HR Wallingford report SR 350, UK.

Roelvink, D., Reniers, A., van Dongeren, A., van Thiel de Vries, J., McCall, R., Lescinski, J., 2009. Modelling storm impacts on beaches, dunes and barrier islands. Coast. Eng. 56 (11-12), 1133–1152.

Saulnier J.B., A. Clement a , A. F. de O. Falcao , T. Pontes, M. Prevosto, P. Ricci. Wave groupiness and spectral bandwidth as relevant parameters for the performance assessment of wave energy converters. Ocean Engineering 38 (2011) 130–147.

Smit, P., Zijlema, M. and Stelling, G., 2013.Depth-induced wave breaking in a non-hydrostatic, near shore wave model. Coast. Engng., 76, 1-16.

Smit, P., Stelling, G., Roelvink, J., Van Thiel de Vries, J., McCall, R., Van Dongeren, A., Zwinkels, C. and Jacobs, R. (2010). XBeach: Nonhydrostatic model: Validation, verification and model description. Tech. rep., Delft University of Technology.

Soares CG (1984) Representation of double-peaked sea wave spectra. Ocean Engineering 11 (2), 185-207.

Strekalov, S.S., Tsyploukhin, V.P., and Massel, S.T., "Structure of Sea Wave Frequency Spectrum", Proc. 13th Coastal Eng. Conference, Volume 1, 1972.

Thompson, D. A., H. Karunarathna and D. E. Reeve “Modelling Extreme Wave Overtopping at Aberystwyth Promenade” by Water 2017, 9(9), 663

Van Hijum, E., Pilarczyk, K., W. 1982. “Equilibrium profile and longshore transport of coarse material under regular and irregular wave attack”. Delft Hyd. Lab. Pub No 274

Van Rijn, L.C., Walstra, D.J.R., Grasmeijer, B., Sutherland, J., Pan, S. and Sierra, J.P., 2003. The predictability of cross-shore bed evolution of sandy beaches at the time scale of storms and seasons using process-based profile models. Coastal Engineering, Vol. 47, p. 295-327.

Van Rijn, L.C., 2006. Principles of sedimentation and erosion engineering in rivers, estuaries and coastal seas. Aqua Publications, The Netherlands (www.aquapublications.nl.

Van Rijn, L.C., 2007. Unified view of sediment transport by currents and waves, IV: Application of morphodynamic model. Journal of Hydraulic Engineering, ASCE, Vol. 133, No. 7, p. 776-793.

Van Wellen, E, Chadwick, A J and Mason, T. 2000. A review and assessment of longshore sediment transport equations for coarse grained beaches. Coastal Engineering, 40, 3, 243-275.

Zijlema, M., Stelling, G. and Smit, P. (2011). Swash: an operational public domain code for simulating wave fields and rapidly varied flows in coastal waters. Coastal Engineering, 58 (10), 992–1012.